PHYSICAL REVIEW D **92,** 103502 (2015)

Scalar field deformations of ΛCDM cosmology

Artur Alho[*]

Center for Mathematical Analysis, Geometry and Dynamical Systems, Instituto Superior Técnico, Universidade de Lisboa, Av. Rovisco Pais, 1049-001 Lisboa, Portugal

Claes Uggla[†]

Department of Physics, Karlstad University, S-651 88 Karlstad, Sweden

(Received 4 August 2015; published 2 November 2015)

This paper treats nonrelativistic matter and a scalar field ϕ with a monotonically decreasing potential minimally coupled to gravity in flat Friedmann-Lemaître-Robertson-Walker cosmology. The field equations are reformulated as a three-dimensional dynamical system on an extended compact state space, complemented with cosmographic diagrams. A dynamical systems analysis provides global dynamical results describing possible asymptotic behavior. It is shown that one should impose *global and asymptotic* bounds on $\lambda = -V^{-1}dV/d\phi$ to obtain viable cosmological models that continuously deform ΛCDM cosmology. In particular we introduce a regularized inverse power-law potential as a simple specific example.

DOI: 10.1103/PhysRevD.92.103502 PACS numbers: 98.80.-k, 95.36.+x, 98.80.Jk, 95.30.Sf

I. INTRODUCTION

Recent observations, such as those of the cosmic background radiation, show that Λ cold dark matter (ΛCDM) cosmology is remarkably consistent with observations, although some tensions remain; see [1,2] and references therein. On the other hand, the unknown origins and nature of dark matter and dark energy remain mysteries which generate a steady flow of models and theories. Nonetheless, current observations should be taken seriously, and viable cosmological models should therefore presumably only deviate from ΛCDM cosmology marginally. Moreover, although successful, the ΛCDM model still needs to be observationally tested, which suggests that it should be continuously deformed. In addition, for a variety of reasons, it is of interest to consider a dynamical dark energy content described by a field theoretical model instead of a cosmological constant Λ or a dark energy fluid. This leads to the question: What phenomenological conditions must be imposed on an effective classical field description of dark energy to continuously deform ΛCDM cosmology for an open set of observationally viable solutions?

Although observational compatibility arguably comes first, there also exist other issues that are of interest such as various fine-tuning problems and if there exist observationally viable models that emerge from, or at least have ties to, a fundamental theory. The rather modest purpose of this paper, however, is to

(i) describe general features and determine asymptotic behavior of flat Friedmann-Lemaître-Robertson-Walker (FLRW) models with a perfect fluid and a scalar field ϕ, minimally coupled to gravity, with a positive monotonic potential $V(\phi)$,
(ii) shed some light on the above "observationally viable field theoretical ΛCDM-deformation issue" by considering some simple models of the above type with the equation of state for the perfect fluid specialized to dust, representing nonrelativistic matter (mainly baryons and nonbaryonic dark matter).

Since the literature about minimally coupled scalar fields and a perfect fluid in a flat FLRW spacetime geometry is vast, we will start with only a few general sample references: the influential papers [3–5] and the recent review [6], and references therein.

It is of interest for discussions and future purposes to first consider a perfect fluid with a general barotropic equation of state $p_m = (\gamma_m - 1)\rho_m$, where p_m and $\rho_m \geq 0$ are the pressure and energy density, respectively, and $\gamma_m = \gamma_m(\rho_m)$, together with a scalar field ϕ, minimally coupled to gravity, with a self-interaction potential $V(\phi)$. Thus, the Einstein and matter field equations for the present flat FLRW models can be written as (see, e.g., [7–9])

$$3H^2 = \frac{1}{2}\dot{\phi}^2 + V(\phi) + \rho_m, \tag{1a}$$

$$\dot{H} = -\frac{1}{2}(\dot{\phi}^2 + \gamma_m\rho_m), \tag{1b}$$

$$0 = \ddot{\phi} + 3H\dot{\phi} + V_\phi, \tag{1c}$$

$$\dot{\rho}_m = -3H\gamma_m\rho_m, \tag{1d}$$

where $V_\phi = dV/d\phi$ and where overdots denote derivatives with respect to cosmic time t. Units are such that

[*]aalho@math.ist.utl.pt
[†]claes.uggla@kau.se

$8\pi G = 1 = c$, where G is the gravitational constant and c the speed of light in vacuum. It is assumed throughout the paper that the Universe is expanding, i.e., $H > 0$.

Equation (1c) can be heuristically interpreted as an equation for a particle of unit mass with a one-dimensional coordinate ϕ, moving in a potential $V(\phi)$ with a friction force $-3H\dot{\phi}$. Equation (1a) shows that H can be expressed in terms of ϕ, $\dot{\phi}$, and ρ_m. Introducing $\dot{\phi}$ as an independent variable therefore leads to a three-dimensional dynamical system for $\phi, \dot{\phi}, \rho_m$. Alternatively one can solve Eq. (1d) to obtain $\rho_m = \rho_m(a)$ and consider the variables $\phi, \dot{\phi}, a$ as the dependent variables, where a obeys the equation $\dot{a} = aH$, where H can be expressed in terms of $\phi, \dot{\phi}, a$ by means of (1a).

It is of some interest to introduce effective equation of state parameters, defined by

$$\gamma_\phi = \frac{\rho_\phi + p_\phi}{\rho_\phi} = \frac{\dot{\phi}^2}{\frac{1}{2}\dot{\phi}^2 + V(\phi)}, \quad \gamma_{\mathrm{tot}} = \frac{\rho_{\mathrm{tot}} + p_{\mathrm{tot}}}{\rho_{\mathrm{tot}}}, \tag{2}$$

or, alternatively, $w_* = p_*/\rho_* = \gamma_* - 1$ $(* = \phi, \mathrm{tot})$, where

$$\rho_\phi = \frac{1}{2}\dot{\phi}^2 + V(\phi), \qquad p_\phi = \frac{1}{2}\dot{\phi}^2 - V(\phi), \tag{3a}$$

$$\rho_{\mathrm{tot}} = \rho_\phi + \rho_m, \qquad p_{\mathrm{tot}} = p_\phi + p_m. \tag{3b}$$

Adding a cosmological constant to a perfect fluid with a barotropic equation of state can be regarded as a problem with a single fluid with a changed barotropic equation of state. Replacing a cosmological constant in a general barotropic fluid description with a scalar field therefore adds the dynamical degrees of freedom, ϕ and $\dot{\phi}$, to ρ_m (or a), which implies a complication, since this leads to a larger set of solutions with different histories. In the context of ΛCDM deformations this problem is somewhat alleviated by the following assumption: To obtain an evolutionary history such that primordial nucleosynthesis gives observationally compatible light nuclear abundances, we will assume that there exists a mechanism such as inflation that sets initial conditions for the present models at high redshifts so that the matter content greatly dominates over the scalar field (dark energy) content in the early Universe.

For simplicity we will from now on consider a linear equation of state with a constant γ_m restricted to the range $0 < \gamma_m < 2$, which avoids bifurcations at $\gamma_m = 0$, corresponding to a cosmological constant, and $\gamma_m = 2$, which yields a stiff perfect fluid with the speed of sound equal to the speed of light; $\gamma_m = 1$ corresponds to a fluid without pressure, which will be the focus when describing and discussing ΛCDM deformations, while $\gamma_m = 4/3$ corresponds to a radiation fluid. It follows from Eq. (1d) that

$$\rho_m = \rho_0 (a/a_0)^{-3\gamma_m}. \tag{4}$$

Furthermore, most of the scalar field potentials that have been considered as possible alternatives to a cosmological constant as dark energy have strictly monotonic scalar field potentials, as exemplified by, e.g., the popular inverse power-law potential. Apart from the model with $V = \Lambda = \mathrm{const.}$, we will therefore assume that V is defined, differentiable, positive, and strictly monotone for $\phi \in (\phi_-, \phi_+)$. Without loss of generality, we assume that V is monotonically decreasing. We also assume that the potential is such that $\phi_+ = \infty$. If ϕ_- is finite or $-\infty$ depends on how fast $V(\phi)$ increases when $\phi \to \phi_-$, e.g., for an inverse power-law potential, $V \propto \phi^{-\alpha}$, $\phi_- = 0$, while an exponential potential, $V \propto \exp(-\lambda\phi)$, leads to $\phi_- = -\infty$.

A constant or monotonically strictly decreasing potential makes it convenient to use a particular type of dynamical systems formulation that brings

$$\lambda(\phi) = -\frac{V_\phi}{V} \tag{5}$$

into focus, where λ is zero for a constant potential and positive for $\phi \in (\phi_-, \infty)$ when $V(\phi)$ is strictly monotonically decreasing. Within this context it is natural to regard λ as more "fundamental" than V itself, where V is obtained from $\lambda(\phi)$ via

$$V = V_0 \exp\left(-\int_{\phi_0}^{\phi} \lambda(\tilde{\phi}) d\tilde{\phi}\right). \tag{6}$$

In the special case where λ and $\lim_{\phi\to\phi_-}\lambda$ are bounded it follows that the potential can be bounded by an exponential and therefore $\phi_- = -\infty$. If λ is unbounded, as in the case of an inverse power-law potential, ϕ_- is finite.

Finally we note that the system (1) has unbounded variables and right-hand sides that blow up. It is therefore not suitable for a global or asymptotic analysis of the solution space and its properties. Below we will therefore make a change of variables in order to obtain a dynamical system on a compact state space that allows these issues to be addressed, as well as giving global illustrative pictures of the entire solution spaces of the models under consideration.[1]

The outline of the paper is as follows. In the next section we (i) formulate the dynamical systems approach that is used throughout the paper to deal with a fluid and a minimally coupled scalar field; (ii) describe the state space features; (iii) point out some global properties and determine asymptotic behavior for models with a perfect fluid and a scalar field such that $0 < \lambda(\phi) < \infty$, $\phi \in (\phi_-, \infty)$, and

[1]For a few examples of work dealing with dynamical systems methods in cosmology, see [7,8,10–15], and references therein.

$$\lim_{\phi\to\infty}\lambda=\lambda_+,\qquad \lim_{\phi\to\phi_-}\lambda=\lambda_-, \tag{7}$$

where λ_+ is finite and λ_- is finite or ∞.

In Sec. III we (i) situate ΛCDM cosmology, which occurs for $\lambda=0$, in the three-dimensional state space, which leads to the concept of an attracting separatrix surface rather than individual "attractor solutions"; (ii) consider the $\lambda=$ const. (i.e., an exponential potential) and dust models in the present context and give a specific example that shows that some of these models are completely solvable; (iii) discuss the symmetries of the above models and how the associated structures might be somewhat misleading for the general picture.

In Sec. IV we turn from the previous "frozen λ" models to some "dynamical λ" models. We consider (i) the inverse power-law potentials, characterized by $\lambda=\alpha/\phi$, in a global dynamical systems setting, tying local results to the global features discussed in Sec. II; in particular we point out that observational viability requires fine-tuning of α to small values, since $\lambda\to\infty$ when $\phi\to 0$ produces a "memory" that affects the entire evolution of, e.g., "tracker" (attractor) solutions. For this reason we therefore (ii) consider the arguably simplest possible "λ-regularization" of the inverse power-law potential, namely, $\lambda=\alpha/\sqrt{C^2+\phi^2}$, which, in contrast to the inverse power-law case, gives rise to continuous deformations of the attracting ΛCDM separatrix surface, and which for $C\gtrsim\alpha$ yields much less stringent observational compatibility conditions on α. Finally, the section is concluded with (iii) a general discussion about observational viability conditions that λ should satisfy for *any* potential that might arise from some fundamental theory.

Throughout we use dynamical systems pictures which clearly display general key features, and, in order to compare with ΛCDM cosmology, these pictures are complemented by diagrams that indicate the evolutionary history of physically important quantities. Finally, we outline how it is possible to treat two fluids, e.g., dust and radiation, and a scalar field in the Appendix.

II. DYNAMICAL SYSTEMS APPROACH

A. Dynamical systems formulation

The presently used dynamical systems formulation is based on the following dependent variables,

$$(x,\Omega_V,\Omega_m,Z)=\left(\frac{\dot\phi}{\sqrt{6}H},\frac{V}{3H^2},\frac{\rho_m}{3H^2},Z(\phi)\right). \tag{8}$$

These variables are by no means suitable for all scalar field potentials, e.g., for potentials with a zero minimum such as monomial potentials it is advisable to replace the scalar field variable Z with an H-based variable that takes into account a varying averaged oscillatory time scale at late times, as done in [15]. Nevertheless, the above variables are useful for positive monotonic potentials. An optimal choice of the variable $Z(\phi)$ depends on the potential that is studied. However, to obtain a suitable global dynamical systems formulation Z should always be chosen to be a globally invertible monotone function in ϕ, defined on a *bounded* interval $Z\in(Z_-,Z_+)$, $Z_\pm=Z(\phi_\pm)$; without loss of generality, we choose Z to be monotonically increasing in ϕ so that $dZ/d\phi>0$ for $Z\in(Z_-,Z_+)$.

Apart from the dependent variables we also need to choose a new time variable. In order to obtain a regular dynamical system this choice depends on if λ is bounded or not. In the case λ is bounded, as exemplified by, e.g., exponentially bounded potentials, it is convenient to use τ, defined by $dt=H^{-1}d\tau$, where $\tau=\ln(a/a_0)$ sometimes is referred to as N, the number of e-folds from a reference time t_0 [$a_0=a(t_0)$], which for the present time leads to $\tau=-\ln(1+z)$, where z is the redshift. Thus, the field equations can be written as the following coupled system:

$$x'=-(2-q)x+\sqrt{\frac{3}{2}}\lambda(Z)\Omega_V, \tag{9a}$$

$$\Omega_m'=3[2x^2-\gamma_m(1-\Omega_m)]\Omega_m, \tag{9b}$$

$$Z'=\sqrt{6}\frac{dZ}{d\phi}x, \tag{9c}$$

where $'$ denotes derivatives with respect to τ. With some slight abuse of notation we have written $\lambda(Z)=\lambda(\phi(Z))=-V_\phi/V$. Furthermore, the Gauss constraint (1a) is used to globally express the Hubble-normalized scalar field potential energy, Ω_V, in terms of the state space variables:

$$\Omega_V=1-x^2-\Omega_m, \tag{10}$$

while the deceleration parameter q, defined via $H'=-(1+q)H$, is given by

$$q=-1+3x^2+\frac{3}{2}\gamma_m\Omega_m. \tag{11}$$

The above system is suitable when λ is bounded, but not when $\lim_{\phi\to\phi_-}\lambda=\infty$, as exemplified by, e.g., inverse power-law potentials. In order to obtain a regular dynamical system when $\lim_{\phi\to\phi_-}\lambda=\infty$ we therefore choose a new time variable $\bar\tau$, defined by $d\tau=g(Z)d\bar\tau$, where $g(Z)$ is a suitable positive bounded function of Z such that $\lim_{Z\to Z_-}g(Z)=0$,

$$\lim_{Z\to Z_-}g_\lambda(Z)=g_{\lambda_-}=\text{const}<\infty,\quad \text{where } g_\lambda(Z)\coloneqq g(Z)\lambda(Z), \tag{12}$$

and $\lim_{Z\to Z_+}g(Z)=1$, where, e.g., $g(Z)=1/(1+\lambda(Z))$ is a suitable choice for inverse power-law potentials. This results in the system

$$\frac{dx}{d\bar{\tau}} = -g(Z)(2-q)x + \sqrt{\frac{3}{2}}g_\lambda(Z)\Omega_V, \tag{13a}$$

$$\frac{d\Omega_m}{d\bar{\tau}} = 3g(Z)[2x^2 - \gamma_m(1-\Omega_m)]\Omega_m, \tag{13b}$$

$$\frac{dZ}{d\bar{\tau}} = \sqrt{6}g(Z)\frac{dZ}{d\phi}x. \tag{13c}$$

Note that (9) is obtained by setting $g(Z) = 1$, hence $\bar{\tau} = \tau$, and so the above system formally covers both cases.

B. State space structures

The above assumptions lead to the following domain for the state vector (x, Ω_m, Z) for the *interior state space* $\mathbf{S}$ for models with a perfect fluid and a scalar field:

$$\Omega_m > 0, \qquad \Omega_V = 1 - x^2 - \Omega_m > 0, \qquad Z_- < Z < Z_+. \tag{14}$$

Furthermore, it follows from (9), and the following auxiliary equation for Ω_V,

$$\Omega_V' = 2\left(1 + q - \sqrt{\frac{3}{2}}\lambda(Z)x\right)\Omega_V, \tag{15}$$

that it is possible to extend the state space and include the following boundaries:

(i) The boundary $\Omega_m = 0$ (i.e., $\rho_m = 0$) yields the (pure) *scalar field boundary subset* [see Eq. (9b)], and thus

$$\Omega_\phi = x^2 + \Omega_V = 1, \tag{16}$$

with an interior state space $\mathbf{S}_\phi$ given by $\Omega_V = 1 - x^2 > 0$, $Z_- < Z < Z_+$.

(ii) The boundary $\Omega_V = 1 - x^2 - \Omega_m = 0$ corresponds to a model with a perfect fluid and a massless scalar field; we refer to this subset as the *massless scalar field boundary subset*. Note that this boundary also contains the pure massless scalar field boundary subset $\Omega_m = 0$, $x = \pm 1$, and the *perfect fluid boundary subset* $\Omega_m = 1$ ($\Omega_\phi = 0$, i.e., $\Omega_V = 0 = x$), which is described by a line of fixed points, FL_Z, with constant Z.

(iii) In addition we assume that the potential and Z are such that the state space $\mathbf{S}$ can be extended to not only include the boundaries $\Omega_m = 0$, $\Omega_V = 0$, but also the boundaries $Z = Z_-$ and $Z = Z_+$, which furthermore are assumed to constitute invariant boundary subsets.

Thus the *extended compact state spaces* $\bar{\mathbf{S}}$ and $\bar{\mathbf{S}}_\phi$ are characterized by

$$\Omega_m \geq 0, \quad \Omega_V = 1 - x^2 - \Omega_m \geq 0, \quad Z_- \leq Z \leq Z_+, \tag{17a}$$

$$\Omega_V = 1 - x^2 \geq 0, \qquad Z_- \leq Z \leq Z_+, \tag{17b}$$

respectively, and the dynamical systems on $\bar{\mathbf{S}}$ and $\bar{\mathbf{S}}_\phi$ are of differentiability class C^1 or higher. We therefore assume that the potential is such that it is possible to find a scalar field variable Z and, if needed, a function $g(Z)$ so that

(i) $g_\lambda(Z)$ *and* $g(Z)dZ/d\phi$ are bounded and differentiable on the extended interval $Z \in [Z_-, Z_+]$,

(ii) $g(Z)dZ/d\phi|_{Z=Z_\pm} = 0$, i.e., $Z = Z_-$ and $Z = Z_+$ are invariant boundary subsets.

Although the above restrictive assumptions require that the potential $V(\phi)$ is of differentiability class C^2, they cover a vast class of potentials $V(\phi)$. Moreover, the extended state space treatment of the admissible class of potentials can be used to provide bounds on asymptotic behavior of potentials that do not admit Z-extended state spaces, and thus they provide a natural starting point for very general situations. It should also be noted that for many qualitative dynamical aspects, as will be seen, there is no need to state any more information about $Z(\phi)$ or $V(\phi)$, although quantitative treatments of course need specific functions and thus we will give specific examples when dealing with continuous ΛCDM deformations.

To physically compare solutions that are obtained in the dynamical systems approach with ΛCDM cosmology, we will complement the state space description with diagrams involving physically important quantities. Apart from the physically important state space variable Ω_m we have given the deceleration parameter q in terms of state space variables in Eq. (11), and below we will also express H in state space variables. In addition it is of interest to give the jerk parameter j [16,17], since even though the observational feasibility of j is questionable, it is still useful in order to theoretically compare models with ΛCDM cosmology for which $j = 1$; for constant γ_m the jerk parameter is given by

$$j = 1 + 9x^2 - \frac{9}{2}\gamma_m(1-\gamma_m)\Omega_m - 3\sqrt{6}\lambda(Z)\Omega_V x. \tag{18}$$

Next we turn to structures that are helpful when it comes to determining global and asymptotic state space features.

C. Nonlocal features

1. The monotonicity of H

The Hubble parameter H, or more conveniently H^2, can be expressed in the state space variables in $\mathbf{S}$ and $\mathbf{S}_\phi$ and is given by

$$H^2 = \frac{V(\phi(Z))}{3\Omega_V} = \frac{V(\phi(Z))}{3(1-x^2-\Omega_m)}, \tag{19}$$

as follows from the definition of Ω_V. This has far-reaching consequences for the global dynamics due to

TABLE I. Table depicting the type of fixed points that can occur for a FLRW model with a monotonically decreasing scalar field potential with a finite λ and a perfect fluid with a linear equation of state parameter $0 < \gamma_m < 2$.

FL	$x = 0,\ \Omega_m = 1$	$q = (3\gamma_m - 2)/2$	$\cdots$
EM	$x = \sqrt{3/2}\gamma_m\lambda^{-1},\ \Omega_m = 1 - 3\gamma_m\lambda^{-2};\ \lambda > \sqrt{3\gamma_m}$	$q = (3\gamma_m - 2)/2$	$\gamma_\phi = \gamma_m$
$M^\pm$	$x = \pm 1,\ \Omega_m = 0$	$q = 2$	$\gamma_\phi = 2$
PL	$x = \lambda/\sqrt{6},\ \Omega_m = 0;\ \lambda < \sqrt{6}$	$q = -1 + \lambda^2/2$	$\gamma_\phi = \lambda^2/3$
dS	$x = \Omega_m = 0;\ \lambda = 0$	$q = -1$	$\gamma_\phi = 0$

$$H' = -(1+q)H \Rightarrow (H^2)' = -2(1+q)H^2, \quad (20)$$

since Eqs. (10) and (11) lead to

$$1 + q = 3x^2 + \frac{3}{2}\gamma_m\Omega_m,$$
$$2 - q = 3\Omega_V + \frac{3}{2}(2-\gamma_m)\Omega_m, \quad (21)$$

which together with $0 < \gamma_m < 2$ yield

$$-1 \le q \le 2. \quad (22)$$

As will be seen, the above inequalities for q, induced by energy and causality conditions, play a central role for the dynamics, which strongly suggests that the field equations should be expressed in terms of q, as done in (9).

The above relations imply that $q = 2$ only occurs on the pure massless scalar field subsets $x = \pm 1$, while $q = -1$ requires $\Omega_m = x = 0, \Omega_V = 1$. Since $1 + q > 0$ on $\mathbf{S}$, H^2 is a monotonically decreasing function on $\mathbf{S}$. This is also true for $\mathbf{S}_\phi$, as can be seen as follows. On $\mathbf{S}_\phi$ we have the inequalities $-1 \le q \le 2$. As a consequence H^2 is a monotonically decreasing function also on this subset, except when $1 + q = 0$. However, when $1 + q = 0$ is not an invariant subset, then $1 + q = 0$ just corresponds to an inflection point in the graph of H^2, and H^2 is thereby still monotonically decreasing.[2] It is only when $1 + q = 0$ is an invariant subset that H^2 stops decreasing and for which $1 + q = 0$ can be an asymptotic state. For this to happen requires that $x = 0$, since $1 + q = 3x^2$ on $\mathbf{S}_\phi$, which also means that $x = 0$ must be an invariant subset. Since $x' = \sqrt{\frac{3}{2}}\lambda(Z)$ when $\Omega_m = 0 = x$, $\Omega_V = 1$, this leads to the condition that $\lambda(Z) = 0$, which by our assumptions about monotonically decreasing potentials can only happen on the $Z_\pm$ boundaries. Hence H^2 is also monotonically decreasing on $\mathbf{S}_\phi$. This implies that there can be no fixed points or recurring orbits (solution trajectories) in $\mathbf{S}$ and $\mathbf{S}_\phi$, and due to (19) all solution trajectories in $\mathbf{S}$ and $\mathbf{S}_\phi$ originate and end at $Z_\pm$ and $\Omega_V = 0$, which shows that it is essential to extend the state space to include these boundaries in order to fully describe the dynamics of the present models.

[2]For an elaboration of this in the case of monomial potentials, see [15].

2. The $Z_\pm$ boundaries

Let us begin by considering the $Z_\pm$ boundaries for the case where $\lim_{Z\to Z_\pm}\lambda = \lambda_\pm$ is finite. Dropping the subscript $\pm$ on $\lambda_\pm$ leads to the system

$$x' = -(2-q)x + \sqrt{\frac{3}{2}}\lambda\Omega_V, \quad (23a)$$

$$\Omega_m' = 3[2x^2 - \gamma_m(1-\Omega_m)]\Omega_m, \quad (23b)$$

on $Z_\pm$ where we recall that $\Omega_V = 1 - x^2 - \Omega_m$ and $q = -1 + 3x^2 + \frac{3}{2}\gamma_m\Omega_m$. As will be elaborated on in the next section, these equations describe the reduced equations of an exponential potential $V \propto \exp(-\lambda\phi)$ when $\lambda \neq 0$ and those of a constant potential when $\lambda = 0$. The above system has an extended state space $\bar{\mathbf{S}}_{\rm red}$ given by

$$\Omega_m \ge 0, \qquad \Omega_V = 1 - x^2 - \Omega_m \ge 0, \quad (24)$$

and admits a number of fixed points given in Table I.

We have here introduced a notation for the fixed points where the kernel M stands for a massless scalar field state; FL stands for a Friedmann-Lemaître perfect fluid state, while dS stands for a de Sitter state (for interpretation of various types of de Sitter states in scalar field cosmology, see [15]); the kernel PL stands for power law (inflation, when $\lambda < \sqrt{2}$, since this leads to an accelerating state with $q < 0$), while EM stands for a scaling solution with an exponential potential and matter in the form of a perfect fluid with a linear equation of state. In addition, a superscript describes the value of x, while in the full three-dimensional treatment we also add a subscript that describes the value for Z.

A one-parameter set of orbits in $\bar{\mathbf{S}}_{\rm red}$ originates from each of the sources M^+ and M^- when $\lambda < \sqrt{6}$, but when $\lambda > \sqrt{6}$ there are no solutions that originate from M^+ into $\mathbf{S}_{\rm red}$, while one solution originates from FL. Toward the future PL is a sink when $\lambda < \sqrt{3\gamma_m}$ while EM is future stable when $\lambda > \sqrt{3\gamma_m}$. Thus bifurcations take place when $\lambda = \sqrt{6}$, which is when PL leaves the physical state space via M^+, and when $\lambda = \sqrt{3\gamma_m}$, which is when EM enters the

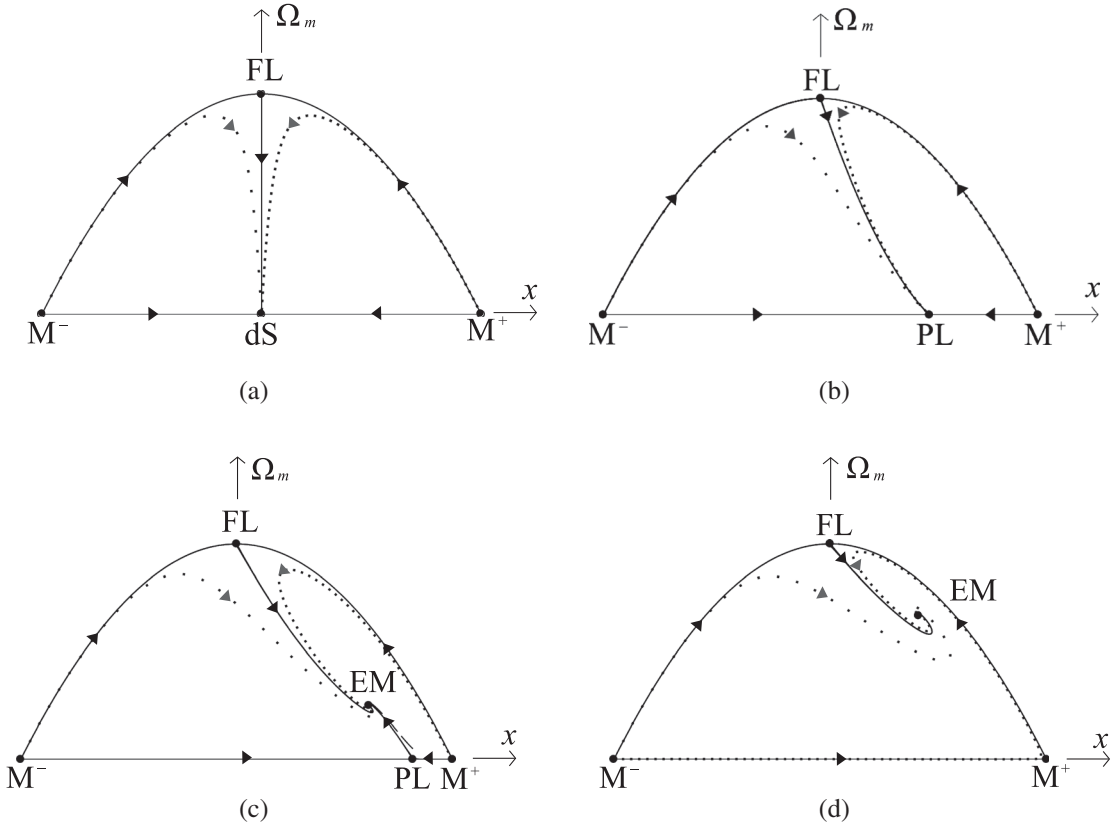

FIG. 1. Representative solution space structures for $\bar{\mathbf{S}}_{\text{red}}$. (a) Solution space for $\lambda = 0$ and $\gamma_m = 1$, (b) Solution space for $\lambda = \sqrt{\frac{3}{2}}$ and $\gamma_m = 1$, (c) Solution space for $\lambda = 2$ and $\gamma_m = 1$, (d) Solution space for $\lambda = 3$ and $\gamma_m = 1$.

state space via PL. In addition there is a bifurcation when $\lambda = 0$, which is when PL becomes the future sink dS. The solution space structures for representative examples of these different cases are given in Fig. 1.

The case when $\lambda \to \infty$ when $\phi \to \phi_-$ yields the following system on Z_-:

$$\frac{dx}{d\bar{\tau}} = \sqrt{\frac{3}{2}} g_{\lambda_-} \Omega_V, \tag{25a}$$

$$\frac{d\Omega_m}{d\bar{\tau}} = 0, \tag{25b}$$

where we recall that $g_{\lambda_-} = \lim_{Z \to Z_-}(g(Z)\lambda(Z)) > 0$. It follows that $\Omega_m = \text{const.}$ while the subset $\Omega_V = 1 - x^2 - \Omega_m = 0$ forms a line of fixed points M^x, and that x is monotonically increasing in $\mathbf{S}_{\text{red}}$. Thus M^x with $x < 0$ is the source while M^x with $x > 0$ is the sink of all orbits in $\mathbf{S}_{\text{red}}$; finally, note that M^x with $x = 0$ is the fixed point FL.

3. The $\Omega_V = 0$ boundary

We first note that the equation for x on $\Omega_V = 0$ is invariant under the transformation $x \to -x$, which enables one to use $\Omega_{\text{stiff}} = x^2$ as a variable instead of x, and as a result, the dynamics of the massless scalar field explicitly takes the same form as that of a stiff fluid, $p = \rho$. This leads to the equations

$$\Omega_m' = 3(2 - \gamma_m)(1 - \Omega_m)\Omega_m, \tag{26a}$$

$$Z' = \sqrt{6}\frac{dZ}{d\phi}x = \pm\sqrt{6}\frac{dZ}{d\phi}\sqrt{1 - \Omega_m}, \tag{26b}$$

where we have used the Gauss constraint to write $\Omega_{\text{stiff}} = 1 - \Omega_m$ and $x = \pm\sqrt{\Omega_{\text{stiff}}}$. Since the equation for Ω_m decouples from that of Z, it follows that all orbits (solution trajectories) in the two-dimensional state space look the same as the orbits of the one-dimensional problem associated with Ω_m, when projected onto Ω_m. As follows from (26a), Ω_m monotonically increases from 0 to 1. Thus the past asymptotic state of all orbits on $\Omega_V = 0$ resides on the pure massless scalar field subset $\Omega_m = 0$, $x^2 = 1$ and thereby $q = 2$; thus either $x = +1$, which from (26b) leads to $Z = Z_-$ and thus a fixed point $\mathrm{M}^+_{Z_-}$, since $dZ/d\phi > 0$, or $x = -1$, which yields $Z = Z_+$ and a fixed point $\mathrm{M}^-_{Z_+}$. It also follows that the future asymptotic state of all orbits on $\Omega_V = 0$ resides on $\Omega_m = 1$, $x = 0$, $Z = \text{const}$, which thereby form a line of fixed points FL_Z. To determine what happens with Z toward the future on $\Omega_V = 0$ we note that it is possible to solve the equation for Ω_m explicitly, but

the solution can also be obtained by using the fact that $\rho_{\rm stiff} \propto \exp(-6\tau)$, $\rho_m \propto \exp(-3\tau)$, $3H^2 = \rho_{\rm stiff} + \rho_m$, which gives

$$\frac{H}{H_0} = (\Omega_{\rm stiff0}\exp(-6\tau) + \Omega_{m0}\exp(-3\gamma_m\tau))^{1/2}, \quad (27a)$$

$$x = \pm\Omega_{\rm stiff0}^{1/2}\exp(-3\tau)/(H/H_0), \quad (27b)$$

$$\Omega_m = \Omega_{m0}\exp(-3\gamma_m\tau)/(H/H_0)^2. \quad (27c)$$

To obtain the solution for Z requires a specification of Z. However, it is easier to obtain Z by integrating the equation for ϕ,

$$\phi' = \sqrt{6}x = \pm(6\Omega_{\rm stiff0})^{1/2}\exp(-3\tau)/(H/H_0), \quad (28)$$

and then inserting the result in the chosen definition of Z. As follows from the above equation, $\phi \to$ const. when $\tau \to +\infty$, and therefore also $Z \to$ const. in this limit; i.e., each point on the line FL_Z attracts one solution with positive and one with negative initial x on the $\Omega_V = 0$ boundary. For a representative depiction of the $\Omega_V = 0$ boundary, see Fig. 3(a).

4. Role of the $\Omega_V = 0$ boundary

To study the neighborhood of $\Omega_V = 0$ we note that

$$\Omega_V^{-1}\Omega_V'|_{\Omega_V=0} = 2\left(1 + q - \sqrt{\frac{3}{2}}\lambda(Z)x\right), \quad (29)$$

and hence

$$\Omega_V^{-1}\Omega_V'|_{\mathrm{M}^{\pm}_{Z_\mp}} = \sqrt{6}(\sqrt{6} \mp \lambda(Z_\mp)),$$
$$\Omega_V^{-1}\Omega_V'|_{\mathrm{FL}_Z} = 3\gamma_m. \quad (30)$$

As a consequence it follows that $\mathrm{M}^-_{Z_+}$ is a source for orbits in $\mathbf{S}$ and $\mathbf{S}_\phi$ as is $\mathrm{M}^+_{Z_-}$ when $\lambda(Z_-) < \sqrt{6}$, but if $\lambda(Z_-) > \sqrt{6}$, then no orbits enter $\mathbf{S}$ or $\mathbf{S}_\phi$ from $\mathrm{M}^+_{Z_-}$[3]; a one-parameter set of orbits, one from each point on FL_Z, enters $\mathbf{S}$, where FL_Z acts as a "transversal saddle line," forming a two-dimensional invariant subset in $\mathbf{S}$. By demanding initial data for which Ω_m is close to 1, this implies the important feature that for *all* the models we consider such solutions can be approximated by this (at least initially) *attracting invariant* surface *subset* of codimension 1 with respect to the state space dimension. We will later contrast this feature with discussions about *single* "attracting" solutions that appear for various models in the literature.

5. Monotonicity of negative x

Further restrictions on the global dynamics of the present models come from Eqs. (9a) and (9c). It follows from (9a) that x is monotonically increasing when $-1 < x < 0$, since then $2 - q > 0$. This in turn implies that if an orbit resides or partly resides in the region $-1 < x < 0$, then the orbit originates from $x = -1$, which due to (9c) and $dZ/d\phi > 0$ implies that the past asymptotic state must be $\mathrm{M}^-_{Z_+}$. Furthermore, the monotonicity of x when $-1 < x < 0$ implies that all orbits in $\mathbf{S}$ and $\mathbf{S}_\phi$ must end at $x \geq 0$.

The equation for x can be written on the following form:

$$x' = -\frac{3}{2}(2 - \gamma_m)x\Omega_m - 3\left(x - \frac{\lambda(Z)}{\sqrt{6}}\right)\Omega_V, \quad (31)$$

which shows that x is monotonically decreasing if $\lambda(Z)/\sqrt{6} < x < 1$. In combination with the above result for x this implies that all orbits in $\mathbf{S}$ and $\mathbf{S}_\phi$ must end at $0 \leq x \leq \lambda(Z)/\sqrt{6}$. However, in order for an orbit to end at $x = 0$ requires that $x = 0$ be an invariant subset. Since

$$x'|_{x=0} = \sqrt{\frac{3}{2}}\lambda(Z)(1 - \Omega_m), \quad (32)$$

and since $\Omega_m = 1$ is the FL_Z subset, it follows that this can only be the case if $\lambda(Z) = 0$, which can only happen on the $Z_\pm$ boundaries for a monotonically strictly decreasing potential. The above equation also shows that x is monotonically increasing when $x = 0$ when $Z_- < Z < Z_+$. Furthermore, since $dZ/d\phi > 0$ it follows from (9c) that Z is monotonically increasing (decreasing) in τ, or $\bar{\tau}$, when $x > 0$ ($x < 0$).

If x is future asymptotically positive it follows that $Z \to Z_+$. However, to exclude or show that any of the orbits from $\mathrm{M}^-_{Z_+}$ end up at dS_{Z_-} if $\lambda_- = 0$ requires more information about the potential. If $\lim_{\phi\to\phi_-} V(\phi) =$ const., then there are solutions that end at Z_-, but if $V \to \infty$ when $\phi \to \phi_-$, there are not. This can be understood by considering (1c). A solution with negative x can be viewed as a particle moving in a direction where the potential is monotonically increasing. At the same time it is losing energy due to the friction force $-3H\dot{\phi}$ until $\dot{\phi} = 0$, but then $\ddot{\phi} = -V_\phi$, where V_ϕ is strictly negative. As a consequence the particle changes direction and $\dot{\phi}$ and thereby also x become positive, and therefore $Z \to Z_+$ toward the future.

Thus all orbits in $\mathbf{S}$ and $\mathbf{S}_\phi$ end at the invariant boundary subset Z_+ when the potential is monotonically decreasing and $V \to \infty$ when $\phi \to \phi_-$, which we for simplicity from

[3]Solutions originating from $\mathrm{M}^-_{Z_+}$ corresponds to "scalar field particles" that come from ∞ moving toward decreasing ϕ, while if $\lambda(Z_-) < \sqrt{6}$ the potential is shallow enough so that scalar field particles also can come from $-\infty$ moving toward increasing ϕ. Solutions originating from FL_Z correspond to scalar field particles that initially lie still at some initial value ϕ and then roll down the potential $V(\phi)$.

now on assume (apart from the case of a constant potential, which is treated separately, all our explicit examples obey these conditions).

6. The role of the Z_- subset

The four dynamically qualitatively different cases on Z_- when $0 \leq \lambda_- < \infty$ lead to different interior dynamics:

(i) When $\lambda_- < \sqrt{3\gamma_m}$, a two-parameter (one-parameter) set of orbits originates from the source $\mathrm{M}^+_{Z_-}$ into $\mathbf{S}$ ($\mathbf{S}_\phi$), while a single orbit originates from PL_{Z_-} into $\mathbf{S}_\phi$.

(ii) When $\sqrt{3\gamma_m} < \lambda_- < \sqrt{6}$, again a two-parameter (one-parameter) set of orbits originates from the source $\mathrm{M}^+_{Z_-}$ into $\mathbf{S}$ ($\mathbf{S}_\phi$), but in this case there is also a one-parameter set (a single orbit) that enters $\mathbf{S}$ ($\mathbf{S}_\phi$) from PL_{Z_-} as well as a single orbit from EM_{Z_-}.

(iii) When $\lambda_- > \sqrt{6}$, a single orbit enters $\mathbf{S}$ from EM_{Z_-}.

(iv) When $\lambda_- = 0$, a two-parameter (one-parameter) set of orbits originates from the source $\mathrm{M}^+_{Z_-}$ into $\mathbf{S}$ ($\mathbf{S}_\phi$), while a single orbit originates from dS_{Z_-} into $\mathbf{S}_\phi$.

When $\lambda_- \to \infty$ at Z_-, there is just one orbit that enters $\mathbf{S}$ from FL_{Z_-}, the so-called tracker or attractor solution. The exclusion of orbits into $\mathbf{S}$ and $\mathbf{S}_\phi$ from the fixed points $\mathrm{M}^x_{Z_-}$ with $x \neq 0$ can be understood as follows: There are no solutions coming from $\mathrm{M}^x_{Z_-}$ when $x < 0$ since Z is decreasing toward the future when $x < 0$. When $x > 0$, it follows that Ω_V is decreasing in the vicinity of $\mathrm{M}^x_{Z_-}$ and hence there are no solutions coming from this part of $\mathrm{M}^x_{Z_-}$ into $\mathbf{S}$ or $\mathbf{S}_\phi$ either. Hence $\mathrm{M}^x_{Z_-}$ with $x = 0$, i.e., FL_{Z_-} is the only fixed point on $\mathrm{M}^x_{Z_-}$ which can give rise to a solution into $\mathbf{S}$, and it does give rise to the tracker solution, which can be established by center manifold theory or by consideration of nearby solutions and continuity, since this fixed point acts as a kind of saddle in the full state space.

7. The role of the Z_+ subset

The only solutions that originate from the Z_+ subset into $\mathbf{S}$ ($\mathbf{S}_\phi$) are those from the source $\mathrm{M}^-_{Z_+}$, from which a two-parameter (one-parameter) set of orbits originates into $\mathbf{S}$ ($\mathbf{S}_\phi$).

For the present monotonically decreasing potentials, all orbits in $\mathbf{S}$ and $\mathbf{S}_\phi$ end at Z_+ as follows when $0 \leq \lambda_+ < \infty$:

(i) When $\lambda_+ < \sqrt{3\gamma_m}$, a two-parameter (one-parameter) set of orbits ends at the global sink PL_{Z_+} from $\mathbf{S}$ ($\mathbf{S}_\phi$).

(ii) When $\sqrt{3\gamma_m} < \lambda_+ < \sqrt{6}$, a two-parameter set of orbits in $\mathbf{S}$ ends at the sink EM_{Z_+}, while a one-parameter set of orbits in $\mathbf{S}_\phi$ ends at PL_{Z_+}.

(iii) When $\lambda_+ > \sqrt{6}$, a two-parameter set of orbits in $\mathbf{S}$ ends at the sink EM_{Z_+}, while a one-parameter set of orbits in $\mathbf{S}_\phi$ ends at $\mathrm{M}^+_{Z_+}$.

(iv) When $\lambda_+ = 0$, a two-parameter (one-parameter) set of orbits ends at the global sink dS_{Z_+} from $\mathbf{S}$ ($\mathbf{S}_\phi$).

8. An additional useful quantity

Finally, consider

$$\xi = \frac{\Omega_m}{\Omega_V}, \tag{33}$$

which obeys

$$\xi' = -\sqrt{6}\left(\sqrt{\frac{3}{2}}\gamma_m - \lambda(Z)x\right)\xi, \tag{34}$$

as follows from (9b) and (15). When $\sqrt{\frac{3}{2}}\gamma_m - \lambda(Z)x > 0$, ξ is monotonically decreasing. For a globally bounded λ such that $\lambda(Z) < \sqrt{\frac{3}{2}}\gamma_m$, it follows that ξ is strictly monotonically decreasing and hence $\xi \to 0$ and thereby $\Omega_m \to 0$ toward the future; i.e., the future dynamics resides on the scalar field subset. Toward the past $\xi \to \infty$ and hence $\Omega_V \to 0$ and as a consequence it follows that the past dynamics asymptotically resides on the $\Omega_V = 0$ subset, which of course is already implied by our previous discussion in a somewhat more complicated manner, which, however, includes more details and general situations.

We will now turn to explicit examples of potentials and a fluid with a dust equation of state, $\gamma_m = 1$. Throughout we will choose scalar field variables so that $Z_- = 0$ and $Z_+ = 1$, so that $\bar{\mathbf{S}}$ is given by

$$\Omega_m \geq 0, \quad \Omega_V = 1 - x^2 - \Omega_m \geq 0, \quad 0 \leq Z \leq 1. \tag{35}$$

It should be pointed out that this type of choice of scalar field variable is by no means an optimal choice for all scalar field potentials that can be dealt with by means of a scalar field variable $Z(\phi)$, as illustrated by the treatment of the generalized Chaplygin gas in [11], where $-1 \leq Z \leq 1$, but choices such that $0 \leq Z \leq 1$ are "good enough" for our present purposes. Since $Z_- = 0$ and $Z_+ = 1$ we will introduce 0 and 1 as subscripts instead of $Z_\pm$ to distinguish fixed points on the two boundaries (in addition we have the subscript Z for the line of fixed points FL_Z and, for a constant potential, the line of fixed points dS_Z).

III. FROZEN λCDM DYNAMICS

Before considering the constant and exponential potentials, let us first recall some facts about ΛCDM cosmology. In their simplest form, the ΛCDM models are solutions of Einstein's equations with (i) a spatially isotropic and homogeneous flat FLRW geometry and (ii) a perfect fluid that has negligible pressure, i.e., dust, representing nonrelativistic matter, and a cosmological

constant Λ. It is useful to describe solutions by the following quantities:

$$H = \dot{a}/a, \tag{36a}$$

$$q = -H^{-2}\left(\frac{\ddot{a}}{a}\right) = -\left(1 + \frac{H'}{H}\right), \tag{36b}$$

$$j = H^{-3}\left(\frac{\dddot{a}}{a}\right) = -q' + q + 2q^2, \tag{36c}$$

$$\Omega_m = \frac{\rho_m}{3H^2}, \tag{36d}$$

$$\Omega_\Lambda = \frac{\Lambda}{3H^2}. \tag{36e}$$

Here the cosmographic (or cosmokinetic) quantities $a(t), H(t), q(t), j(t)$ are the cosmological scale factor and the time-dependent Hubble, deceleration, and jerk parameters, respectively [16,17], which take the following form for the ΛCDM models:

$$\frac{H}{H_0} = \sqrt{\Omega_{m0}\exp(-3\tau) + \Omega_{\Lambda 0}}, \tag{37a}$$

$$\begin{aligned} q &= -1 + \frac{3}{2}\Omega_m \\ &= -1 + \frac{3}{2}\left(\frac{\Omega_{m0}\exp(-3\tau)}{\Omega_{m0}\exp(-3\tau) + \Omega_{\Lambda 0}}\right), \end{aligned} \tag{37b}$$

$$j = 1, \tag{37c}$$

$$\Omega_m = \frac{\Omega_{m0}\exp(-3\tau)}{\Omega_{m0}\exp(-3\tau) + \Omega_{\Lambda 0}}, \tag{37d}$$

$$\Omega_\Lambda = \frac{\Omega_{\Lambda 0}}{\Omega_{m0}\exp(-3\tau) + \Omega_{\Lambda 0}}, \tag{37e}$$

where $\Omega_m + \Omega_\Lambda = 1$ and where H_0, Ω_{m0}, and $\Omega_{\Lambda 0}$ are the values of H, Ω_m, and Ω_Λ at the reference time t_0 and hence $\tau = 0$.[4] Throughout we will use the following present values:

$$\Omega_{m0} = 0.3, \qquad \Omega_{\Lambda 0} = 0.7. \tag{38}$$

It follows from (37b) that $q_0 = -0.55$.

Figure 2 depicts the evolution of H/H_0, q, and Ω_m in terms of the redshift z for the ΛCDM models with the above present values. As can be seen, Ω_m monotonically decreases from 1 (corresponding to the big bang limit $\tau \to -\infty$) to zero (corresponding to the infinite future limit $\tau \to +\infty$, described by a de Sitter state with $\Omega_\Lambda = 1$). Alternatively this also follows by considering the differential equation for Ω_m, which is given by (see, e.g., p. 62 in [7])

$$\Omega_m' = -3(1 - \Omega_m)\Omega_m. \tag{39}$$

A. ΛCDM dynamics as $\lambda = 0$-CDM dynamics

Setting $p_m = 0$ and $V = \Lambda$ yields a model that can be interpreted as that of dust, a massless scalar field, and a cosmological constant Λ. The associated model does not solve any of the issues one might find unattractive with the ΛCDM model, but it does show some aspects that are important in a broader context. Since $\lambda = 0$, one obtains a reduced coupled two-dimensional system for x and Ω_m, while the decoupled equation for Z can be integrated once the evolution for x and Ω_m is found. However, instead of just considering the essential reduced extended two-dimensional state space $\bar{\mathbf{S}}_{\text{red}}$, we need to consider the full three-dimensional extended state space $\bar{\mathbf{S}}$ to illustrate how this model is connected with more general models for which $\lambda = \lambda(Z)$. Note, however, that the decoupling of the equation for Z from the coupled system of x and Ω_m results in that all solutions with the same initial data of x and Ω_m yield the same curves when projected onto the $x - \Omega_m$-plane, irrespective of the initial value of Z. To proceed requires that Z be specified. There are many possible choices that lead to an analytic dynamical system on a compact state space that cover the domain $\phi_\pm = \pm\infty$, but here, due to future purposes, we choose

$$Z = \frac{1}{1 + \exp(-\lambda\phi)}, \tag{40}$$

which is monotonically increasing in ϕ and where λ is an arbitrary positive constant; the scalar field variable Z thereby has an extended range $Z \in [0, 1]$. This leads to the following dynamical system for the present models:

$$x' = -(2 - q)x, \tag{41a}$$

$$\Omega_m' = 3[2x^2 - (1 - \Omega_m)]\Omega_m, \tag{41b}$$

$$Z' = \sqrt{6}\lambda Z(1 - Z)x, \tag{41c}$$

[4]Due to noisy data, the current observational feasibility of the jerk parameter j is questionable. Nevertheless, the fact that $j = 1$ for the ΛCDM models makes it useful as a theoretical indicator of deviations from ΛCDM cosmology, and it is for this reason we give j. Moreover, as will be seen, the jerk parameter seems to be the parameter that is most sensitive when it comes to deviations from ΛCDM cosmology; it is unfortunate that it is also the most difficult quantity to observationally measure of the presently discussed ones.

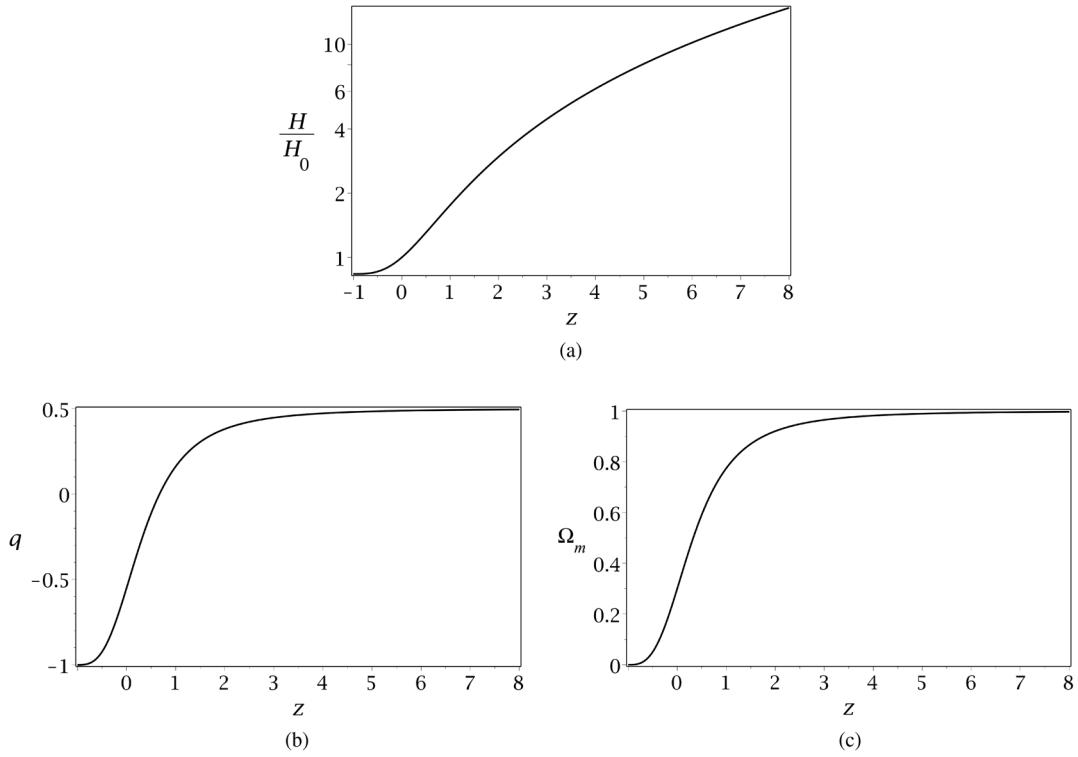

FIG. 2. Depiction of the evolutionary history of ΛCDM cosmology for $\Omega_{m0} = 0.3$, $\Omega_{\Lambda 0} = 0.7$ in terms of the redshift z. (a) $H(z)$-diagram for the ΛCDM models, (b) $q(z)$-diagram for the ΛCDM models, (c) $\Omega_m(z)$-diagram for the ΛCDM models.

where $2 - q = 3(1 - x^2) - \frac{3}{2}\Omega_m = 3(1 - x^2 - \Omega_m) + \frac{3}{2}\Omega_m$. The reduced coupled system for x and Ω_m is invariant under the transformation $x \to -x$, which makes it possible to identify this problem with that of a stiff fluid, characterized by $\Omega_{\text{stiff}} = x^2$, a cosmological constant, and dust. In a similar manner as for the $\Omega_V = 0$ subset, this leads to

$$\frac{H}{H_0} = (\Omega_{\text{stiff}0} \exp(-6\tau) + \Omega_{\Lambda 0} + \Omega_{m0} \exp(-3\tau))^{1/2}, \tag{42a}$$

$$x = \pm\sqrt{\Omega_{\text{stiff}0}} \exp(-3\tau)/(H/H_0), \tag{42b}$$

$$\Omega_m = \Omega_{m0} \exp(-3\tau)/(H/H_0)^2. \tag{42c}$$

As for the $\Omega_V = 0$ subset it is easiest to obtain Z by integrating the equation for ϕ, given by

$$\phi' = \sqrt{6}x = \pm(6\Omega_{\text{stiff}0})^{1/2} \exp(-3\tau)/(H/H_0), \tag{43}$$

and then inserting the solution into (40).

We have previously dealt with the global dynamics of monotonically decreasing potentials. We here give a complete description for the constant potential. The past and future states of all orbits follow from the exact solution, or from the monotone function H^2 in combination with the dynamical structure at the boundaries and the local properties of the fixed points. The result is that a two-parameter set of orbits in $\mathbf{S}$ and a one-parameter set in $\mathbf{S}_\phi$ originate from each of the hyperbolic sources M_0^+ and M_1^-, while a one-parameter set of solutions originates from the transversally hyperbolic line of fixed points FL_Z into $\mathbf{S}$; orbits in $\mathbf{S}$ and $\mathbf{S}_\phi$ end at the transversally hyperbolic line of fixed points dS_Z, which thereby constitute the future attractor. The orbits that come from M_0^+ (M_1^-) correspond to solutions with increasing (decreasing) ϕ from $\phi \to -\infty$ ($\phi \to +\infty$), starting from a massless state [heuristically this can be understood from Eq. (1c) where the friction force $-3H\dot{\phi}$ generates energy toward the past, making the energy content of Λ (and ρ) negligible compared to the kinetic energy of the scalar field], while solutions that originate from FL_Z reside on the invariant subset $x = 0$.

Since the $x = 0$ subset corresponds to solutions with different constant ϕ, and thereby also a constant $\rho_\phi = \Lambda$, these models are identical to the ΛCDM models. We therefore denote the $x = 0$ invariant subset surface as the ΛCDM surface or subset. Furthermore, this surface divides the state space into two disconnected domains with $x > 0$ and $x < 0$, respectively, and the ΛCDM subset thereby acts as a separatrix surface. Note that it is a necessary condition that the potential is a constant for $x = 0$ to be an invariant subset in $\mathbf{S}$ and thus no other potentials yield a ΛCDM model.

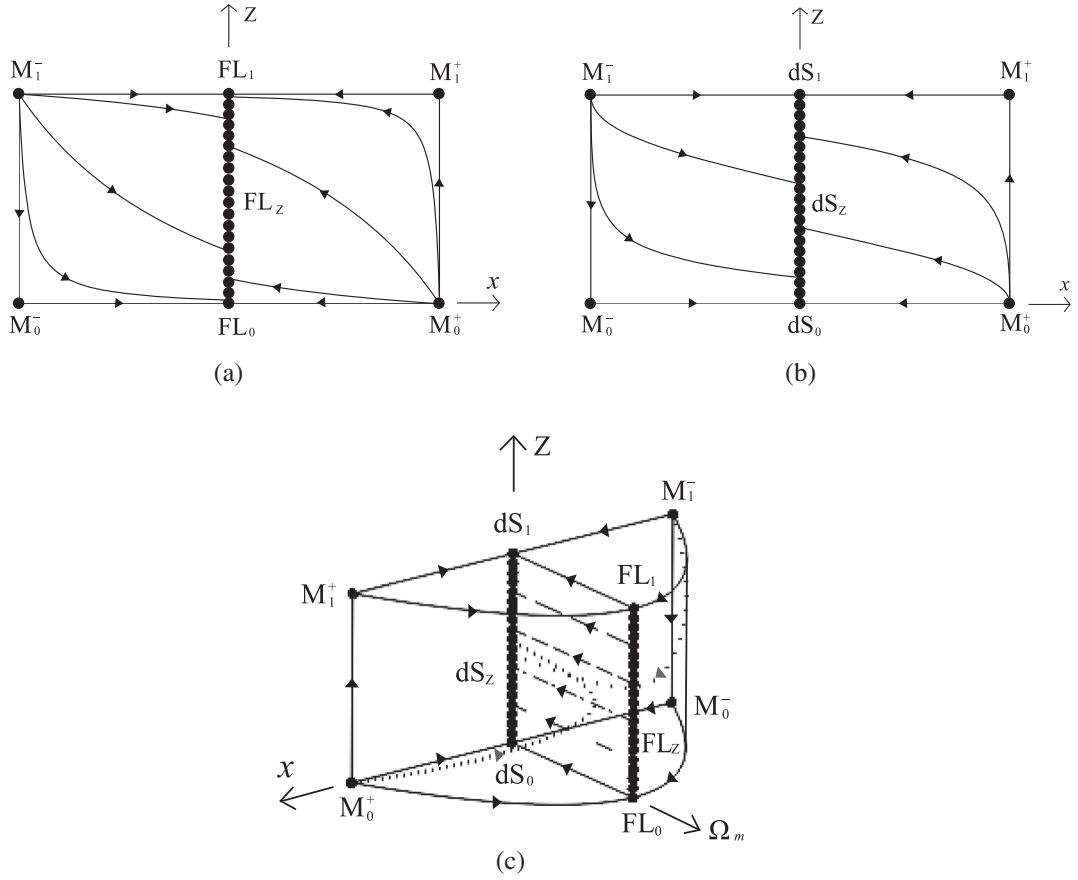

FIG. 3. Depiction of the solution space of a fluid without pressure and a scalar field with a constant potential $V(\phi) = \Lambda > 0$, where $Z = (1 + \exp(-\sqrt{3/2}\phi))^{-1}$, illustrating the $x = 0$ ΛCDM separatrix surface subset and its attracting nature. (a) The massless scalar field boundary $\Omega_V = 0$, (b) The scalar field boundary $\Omega_m = 0$, (c) The (x, Ω_m, Z) state space for a constant potential and dust.

Due to the regularity of the dynamical system and that each fixed point on FL_Z acts as a transversal saddle point (exemplifying the previous general discussion concerning the $\Omega_V = 0$ subset and the vicinity of $\Omega_V = 0$ and FL_Z), and since dS_Z is the future attractor, it follows that the ΛCDM separatrix surface $x = 0$ is an "attracting" surface or invariant subset (indeed, x^2 is monotonically decreasing). As a consequence, demanding that Ω_m be close to 1 initially leads to solutions with almost ΛCDM behavior. The solution space for this set of models is depicted in Fig. 3 where we have chosen $\lambda = \sqrt{3/2}$. Note that the structure on the $\Omega_V = 0$ subset is qualitatively the same for all the potentials we consider, as discussed in the previous section.

The present models in effect do not really have a *dynamical* dark energy since the dark energy content "freezes" toward an "unnatural" value $\Lambda > 0$ toward the future for models with $x \neq 0$, and they therefore do not solve any coincidence or energy scale problems one might have with the ΛCDM models. Nevertheless, since models with Ω_m close to 1 as an initial condition basically have the same evolution as the ΛCDM models, these models with their *attracting* ΛCDM *separatrix surface subset*, in an evolutionary history sense, are the best a scalar field and dust model can accomplish when it comes to mimicking ΛCDM cosmology, and they therefore, from a purely time development perspective, set the standards for any truly dynamical dark energy model. Next we turn to the well-known case of an exponential potential (see, e.g., [18,19]), but in the present three-dimensional context.

B. Constant λ λCDM dynamics

An exponential potential

$$V = V_0 \exp(-\lambda\phi), \qquad \lambda > 0, \tag{44}$$

and a dust matter equation of state results in the dynamical system

$$x' = -(2 - q)x + \sqrt{\frac{3}{2}}\lambda(1 - x^2 - \Omega_m), \tag{45a}$$

$$\Omega_m' = 3[2x^2 - (1 - \Omega_m)]\Omega_m, \tag{45b}$$

$$Z' = \sqrt{6}\lambda Z(1 - Z)x, \tag{45c}$$

where we have used the definition (40) for Z [also, recall that $2-q=3(1-x^2)-\frac{3}{2}\Omega_m$]. Once again there is a decoupling between the scalar field variable Z and a coupled system for x and Ω_m on a reduced state space $\mathbf{S}_{\mathrm{red}}$, parametrized by λ. As for a constant potential, it therefore follows that solutions with the same initial x and Ω_m, but with different initial Z, have the same trajectories when projected onto the $x-\Omega_m$-plane.

The qualitative structure of the solution space of $\bar{\mathbf{S}}$ is entirely determined by the general monotonic features and the structures on the boundary subsets of $\mathbf{S}$ and their neighborhoods described earlier. Thus there are two-parameter sets of orbits in $\mathbf{S}$ that originate from the sources M_0^+ and M_1^- when $\lambda<\sqrt{6}$, but only from M_1^- when $\lambda>\sqrt{6}$, while a one-parameter set of solutions originates from the transversally hyperbolic line of fixed points FL_Z. Toward the future PL_1 is a sink when $\lambda<\sqrt{3}$ (and the future attractor on $\mathbf{S}$ and $\mathbf{S}_\phi$) while EM_1 is future stable when $\lambda>\sqrt{3}$ (and the future attractor on $\mathbf{S}$). As previously shown, it is a general feature that there is a one-parameter set of solutions that originate from the line FL_Z, forming an attracting invariant subset, but it is only when $\lambda<\sqrt{3}$ that this invariant subset forms an "attracting *separatrix* surface," which in the limit $\lambda\to 0$ leads to the previous ΛCDM surface.

It is of historical interest to point out that it was the case with $\lambda>\sqrt{6}$ with EM_1 as the future attractor (although in the two-dimensional projected context) that was the original role model for concepts such as attractor (the fixed point EM_1 *is* the formal future attractor) and tracker solutions in scalar field cosmology [recall that $\gamma_\phi=\gamma_m$ for general γ_m (see Table I); i.e., the effective scalar field equation of state "tracks" the matter equation of state]. As we will see, this is rather misleading. Moreover, from current observational constraints these models are no longer viable cosmological models since $q=1/2$ for the future attractor EM_1. Since models with small λ are arguably more relevant for understanding more general and observationally competitive scalar field models, we focus on this class of models next.

It is worthwhile to point out that since this does not seem to be generally known, there are models with a perfect fluid and a scalar field with an exponential potential that admits simple explicit solutions, as shown by Uggla *et al.* in [20] (where many other solvable scalar field and modified gravity models can be found as well). One such example is for dust when $\lambda=\sqrt{3/2}$. Using the methods in [20], we see that x and Ω_m can be found in terms of cosmological time t:

$$x=\frac{2t^3-c}{4t^3+6t+c},\qquad \Omega_m=\frac{1-x^2}{1+t^2}=\frac{12t(t^3+3t+c)}{(4t^3+6t+c)^2}, \tag{46}$$

which thus explicitly gives the trajectories in the $x-\Omega_m$-plane in parametrized form, where the constant c characterizes the different solutions, with $c=0$ yielding the separatrix subset, i.e., the heteroclinic orbits from FL_Z to PL_1 in $\mathbf{S}$ (a heteroclinic orbit is a solution trajectory that connects two distinct fixed points). The solution space structure is depicted in Fig. 4 [see also the reduced state space in Fig. 1(b)].

Let us now consider the interior solutions in Fig. 4(b) with $\lambda=\sqrt{3/2}$ in an Ω_m-q diagram and in several *cosmographic diagrams* (see Fig. 5), together with the ΛCDM model with $\Omega_{m0}=0.3$ and $\Omega_{\Lambda 0}=0.7$. To have a feeling for the evolution in terms of redshift one can compare with the graphs in Fig. 2, which gives a good estimate for the history also for the other solutions when expressed in the redshift z, as long as they are close to the ΛCDM model. As can be seen, these models are deviating rather significantly from the ΛCDM model, and therefore a considerably smaller value of λ is needed to obtain an evolution that is close to ΛCDM dynamics, even when Ω_m is close to 1 initially. Furthermore, in a certain sense,

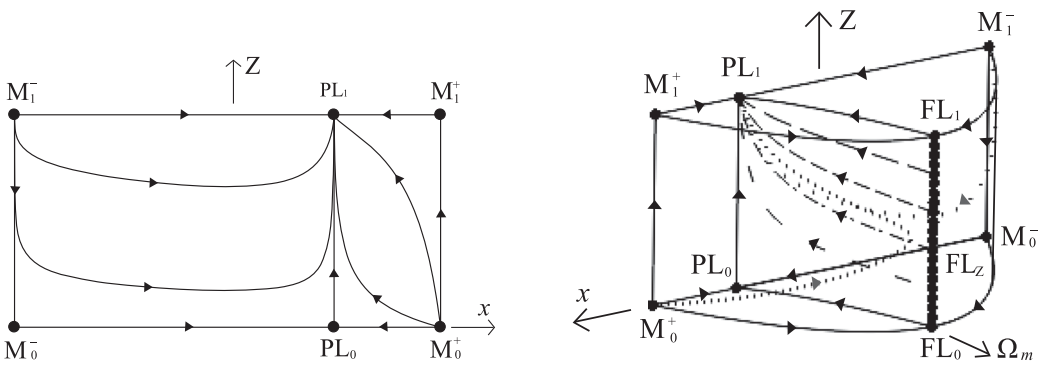

FIG. 4. State space structures for dust and $V=V_0\exp(-\lambda\phi)$ with $\lambda=\sqrt{3/2}$. (a) The scalar field boundary $\Omega_m=0$; $\lambda=\sqrt{3/2}$, (b) The (x,Ω_m,Z) space for dust and $\lambda=\sqrt{3/2}$.

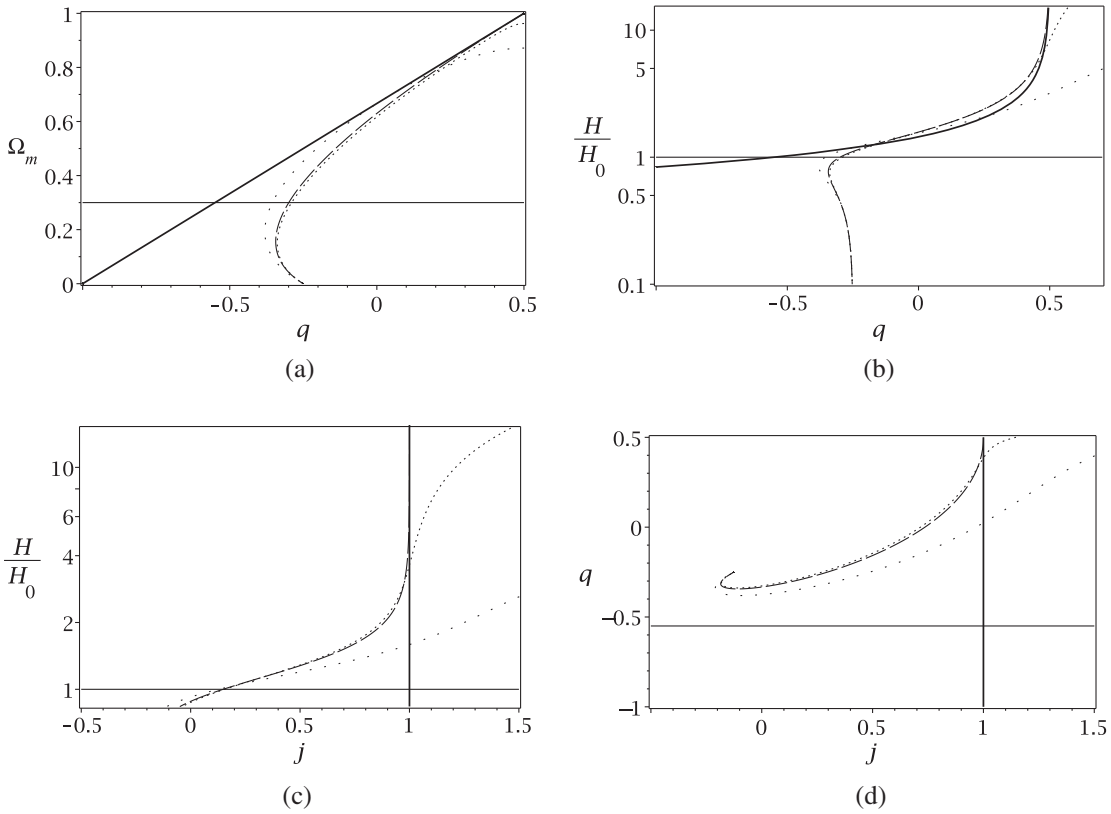

FIG. 5. Diagrams for the observable Ω_m and the cosmographic parameters H, q, j (the Hubble, deceleration, and jerk parameters) for dust and a potential $V = V_0 \exp(-\sqrt{3/2}\phi)$ for the solutions (with the same notation) in Fig. 4(b). The thick line represents ΛCDM cosmology with $\Omega_{m0} = 0.3$, $\Omega_{\Lambda 0} = 0.7$. The horizontal lines with $\Omega_m = 0.3$, $H/H_0 = 1$, and $q = -0.55$ represent the present situation, i.e., $z = 0$. (a) $\Omega_m - q$ diagram, (b) $H - q$ diagram, (c) $H - j$ diagram, (d) $q - j$ diagram.

discussed next, the present class of models is as special as the scalar field models with a cosmological constant, and they are therefore unlikely candidates for solving any of the issues one might have with ΛCDM cosmology.

C. Symmetries of frozen λCDM dynamics

It is only the cases of a constant or an exponential potential that effectively reduce the problem from three to two dimensions by decoupling the equation for the scalar field variable. The underlying reason for this is that these models admit scaling symmetries.

In the case of an exponential potential, a translation of the scalar field leads to a scaling of the potential, which in combination with an appropriate scaling of t yields a scaling of ρ_ϕ; furthermore, a scaling of the spatial coordinates leads to a scaling of the scale factor a and thereby also of ρ_m in the case of a linear equation of state with $\gamma_m \neq 0$, which results in a scaling symmetry of Einstein's field equations. This in turn gives rise to a one-parameter set of equivalent solutions, being the reason for the decoupling property, and it is also the underlying reason for why there exist "scaling solutions," which more appropriately should be referred to as homothetic self-similar solutions since the spacetime geometry of these solutions admits a homothetic Killing vector field. For models with both a perfect fluid with a linear equation of state and a scalar field with an exponential potential, a scaling solution can only exist if ρ_m and ρ_ϕ behave in the same manner, which requires $\gamma_m = \gamma_\phi$. The existence of a fixed point EM on the reduced state space $x - \Omega_m$ therefore necessarily depends on this feature, but it turns out to not always be possible since EM only exists when $\lambda > \sqrt{3\gamma_m}$; furthermore, the *global* attractive property of EM, which does *not* follow from a fixed point analysis, follows from a monotone function that can be *derived* from another kind of symmetry of the field equations that is associated with coordinate scalings (this is a general mechanism, discussed for anisotropic models and perfect fluids in [21]). For a constant potential, scalings of the coordinates instead bring a solution with a given $V = \Lambda$ to a solution with a different Λ, and because Λ carries dimension (length^{-2}), there are no solutions admitting a homothetic symmetry when $\Lambda \neq 0$; i.e., this scaling symmetry is not quite the same as that in the exponential case.

The existence of symmetries is what makes these models tractable and therefore also popular. However, the symmetries endow these models with special properties, which suggests that perhaps it is not a good idea to consider these models as role models, since other models

do not admit similar symmetries and properties, or at least that some careful considerations may be needed. Moreover, originally, before one realized that the deceleration parameter q is evolving, it was thought that scale invariance and thereby a constant q was quite desirable, since this would solve fine-tuning problems such as coincidence and energy scale problems. On the other hand, the symmetries also make the models quite inflexible. Due to the changing evolutionary history of q, where q is currently negative, the scaling symmetries must be broken, while still leading to models that in some way at least alleviate various fine-tuning problems; for these reasons, and from a phenomenological perspective, scale-invariant models are no longer the favorite candidates as dark energy models.

IV. DYNAMICAL λCDM DYNAMICS

A. Inverse power-law potentials

In the influential papers [3,4] Peebles and Ratra argued that dark energy can be phenomenologically modeled by a minimally coupled scalar field with a potential with a shallow tail, which results in the dark field energy density decreasing more slowly than the matter energy density to its "natural" value—zero. In particular they considered an inverse power-law potential,

$$V=\frac{V_0}{\phi^\alpha},\qquad \phi>0,\qquad \alpha>0\Rightarrow\lambda=\frac{\alpha}{\phi}. \tag{47}$$

In addition they assumed a matter dominated flat FLRW universe after inflation, which resulted in a set of approximate flat FLRW equations for which they found a particular solution, which was shown to be linearly stable within the approximate context. The associated solution of the exact FLRW equations has subsequently been referred to as an attractor or tracker solution [5], and has resulted in numerous papers. In [13] a thorough local dynamical systems analysis of the present models was performed, based on previous work, e.g., [22–24] (for additional references see, e.g., [6,13]). Here we will use a slight variation of this approach and use the following bounded scalar field variable:

$$Z=\frac{1}{1+\lambda}=\frac{\phi}{\phi+\alpha}\Rightarrow\lambda=\frac{1-Z}{Z},\qquad \phi=\alpha\left(\frac{Z}{1-Z}\right), \tag{48}$$

where Z thereby is monotonically increasing in ϕ (in [13] $1-Z$ was used as the scalar field variable).

The present case has an unbounded λ, and therefore we use the dynamical system (13), where we choose $g(Z)=Z$, and thus $g_{\lambda_-}=1$ and

$$\frac{d\tau}{d\bar\tau}=Z,\qquad \frac{dt}{d\bar\tau}=H^{-1}Z, \tag{49}$$

and the following dynamical system for the state vector (x,Ω_m,Z):

$$\frac{dx}{d\bar\tau}=-(2-q)xZ+\sqrt{\frac{3}{2}}(1-Z)(1-x^2-\Omega_m), \tag{50a}$$

$$\frac{d\Omega_m}{d\bar\tau}=3[2x^2-(1-\Omega_m)]\Omega_m Z, \tag{50b}$$

$$\frac{dZ}{d\bar\tau}=\frac{\sqrt{6}}{\alpha}(1-Z)^2Zx, \tag{50c}$$

where $2-q=3(1-x^2)-\frac{3}{2}\Omega_m$.

Due to the discussion about global dynamics in Sec. II, it follows that the conclusions obtained from the local fixed point results in [13] correspond to global asymptotic features. Hence a two-parameter set of solutions originates from M_1^-, and a one-parameter set from FL_Z, where the tracker solution originates from FL_0. Toward the future all orbits on $\mathbf{S}$ and $\mathbf{S}_\phi$ end at the global future attractor dS_1.[5] The solution structure for $\alpha=6$, and especially that of the subset that originates from FL_Z, is depicted in Fig. 6.

It is of some interest to complement the dynamical systems picture with a heuristic description where we regard the scalar field as a particle moving in a potential, while losing energy due to the friction force $-3H\dot\phi$. Due to the existence of a potential wall that is so steep that $\lambda\to\infty$ when $\phi\to 0$, all "scalar field particles" (solutions) either come from $\phi\to-\infty$ and bounce against the potential wall (the two-parameter set of solutions from M_1^-) or from being initially still at some ϕ (no initial kinetic scalar field energy, i.e., $x=0$) and then rolling down the potential in the positive ϕ-direction; the tracker solution corresponds to the solution that starts by being initially still with an infinite scalar field energy associated with the limit $\phi\to 0$ (note that this result also follows from the asymptotic explicit results concerning this solution given originally in [3,4]).

All solutions therefore eventually move in an increasingly shallow potential, slowed by "friction," and hence with decreasing scalar field energy, although the matter energy decreases faster, thus leading to a future asymptotic (quasi) de Sitter state at $\phi\to+\infty$ (i.e., dS_1).

Loosely speaking, the tracker solution is connected with a bifurcation associated with going from a potential with finite λ to infinite λ, transforming the attracting focus of the exponential case with large λ to a center. The orbits on

[5]Since $\lim_{\phi\to+\infty}V(\phi)=0$ it follows that the future asymptotic state dS_1 now corresponds to the Minkowski spacetime instead of the de Sitter spacetime. However, because the matter energy density goes to zero faster than the scalar field energy density, it still follows that $q\to-1$; the asymptotic evolution thus resembles that of the de Sitter spacetime, since asymptotically the spacetime approaches that of a Minkowski spacetime in a (local) foliation where $q\to-1$. A similar statement holds for the models in the next subsection.

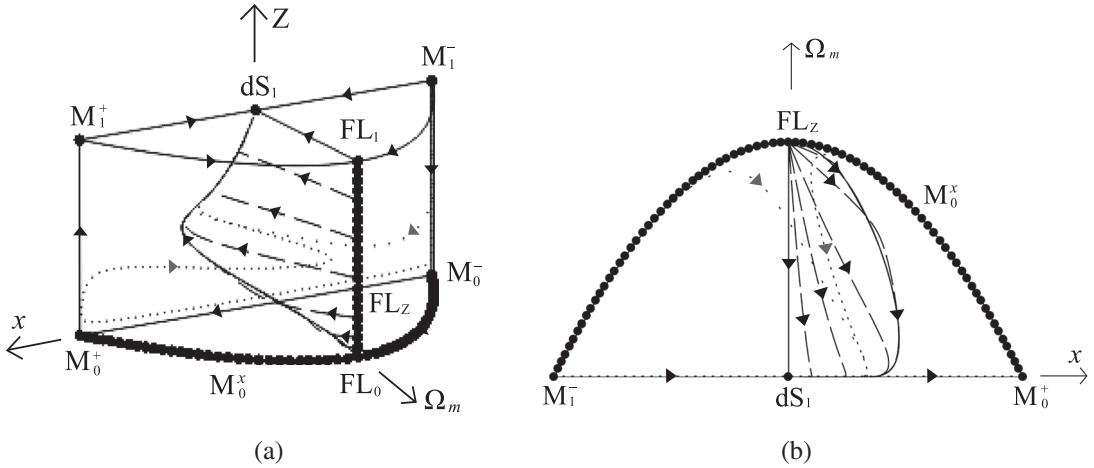

FIG. 6. Solution structure for the state space for models with dust and a scalar field with inverse power-law potential $V = V_0\phi^{-\alpha}$ with $\alpha = 6$. (a) The (x, Ω_m, Z) state space, (b) Projection of (x, Ω_m, Z) state onto (x, Ω_m).

$Z = 0$ are characterized by $\Omega_m = \text{const}$. They therefore correspond to the periodic orbits found in the monomial case at late times, given in different variables in [15], but in the present case they are interrupted by being cut in half by the line of fixed points, M_0^x, which is a formal consequence of the new time variable. The physical reason for this feature is that in contrast to the monomial case there are no scalar field oscillations at late times for inverse power-law potentials.

As can be seen from Fig. 6, the tracker solution forms part of the boundary of the FL_Z saddle subset, which therefore is not a separatrix surface. Because of its initial linear stability property in the Peebles-Ratra formulation [3,4], which was seen as alleviating the coincidence problem, nearby solutions are attracted to it. However, there exists an open set of solutions that are further away from it that are not, even if Ω_m is close to 1 initially (those with fairly large initial Z). This is to be expected since the Peebles-Ratra stability analysis is only local. It should also be pointed out that there is no *a priori* reason for believing that the local attracting property holds globally in time.[6] However, all solutions near the tracker solution, indeed all solutions that are near or on the subset that originates from FL_Z, are eventually shadowing the center manifold of the fixed point dS_1 on $\mathbf{S}_\phi$[7] and it is the center manifold solution on $\mathbf{S}_\phi$ that is an "attractor solution" rather than the tracker solution, since any solution close to this solution is attracted to it because it is a center manifold, but note that it is dS_1 that is the formal future attractor.

As seen from Fig. 6, the tracker solution and the solutions that are near to it on the subset that originates from FL_Z are those solutions on this subset that diverge from ΛCDM dynamics the most (in this sense they are the observationally worst solutions in this subset of solutions, which is also seen by plotting the solutions in diagrams for the observables; see Fig. 7) and quite substantially when $\alpha = 6$. Let us therefore consider the dynamics for models with lower α.

The solution structure for $\alpha = 1/2$, and especially that of the subset that originates from FL_Z, is depicted in Fig. 8. The topological structure is the same as for $\alpha = 6$, but the subset that originates from FL_Z is now located closer to the $x = 0$-plane and as a consequence the dynamics of solutions with Ω_m close to 1 initially more closely resembles that of the ΛCDM models. These results are therefore in line with the conclusion in [6], that it is only for quite small α that the tracker solution is observationally viable, which restricts the observational relevance of these models. The deviations from ΛCDM cosmology can be explicitly seen in the diagrams for the observables in Fig. 9.

Note that Figs. 6 and 8 also show that it is not only the tracker solution that attracts nearby solutions, but the whole FL_Z saddle subset. The underlying reasons for this are that (i) the whole line of fixed points FL_Z acts as a line of saddle points, and (ii) all solutions in this subset are attracted to the center manifold of dS_1 at late times before asymptotically approaching the global future attractor dS_1.

Finally, it is worth noting that the underlying reason for why the early behavior of the tracker solution exhibits a "tracking property" is because the present case can be viewed as a bifurcation where EM_0 merges with FL_0 in the limit $\lambda \to \infty$. The property that $\gamma_\phi = \gamma_m = 1$ for EM, irrespective of λ (as long as EM exists until it merges with PL), can subsequently be exploited by comparing the reduced two-dimensional dynamics of a sequence of

[6]See, e.g., [11] for an example of an attracting solution that is locally but not globally attracting.

[7]Incidentally, it is the center manifold solution on $\mathbf{S}_\phi$ that the slow-roll approximation, given in, e.g., [9], describes approximately; see [14,15] for a similar situation at early times instead of late times.

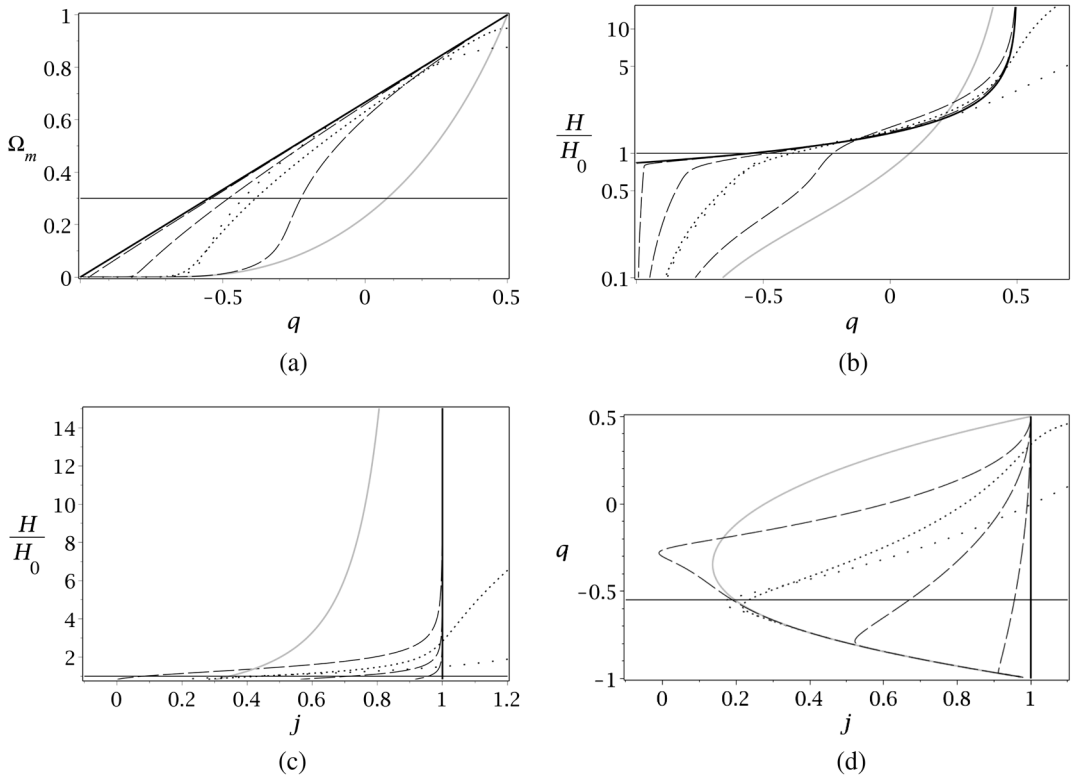

FIG. 7. Observables for dust and an inverse power-law potential $V = V_0\phi^{-\alpha}$ with $\alpha = 6$. The thick solid line represents ΛCDM cosmology; the horizontal lines represent now, i.e., zero redshift; and the other lines correspond to the solutions in Fig. 6, where the grey line corresponds to the tracker solution. (a) $\Omega_m - q$ diagram, (b) $h - q$ diagram, (c) $h - j$ diagram, (d) $q - j$ diagram.

reduced exponential scalar field state spaces, as done in [13,22,23], to yield an approximate heuristic description of the behavior of the tracking solution. Nevertheless, it should be clear that the dynamics of an inverse power-law potential model is globally very different from that of a given exponential potential, which is what can be expected from a model that does not exhibit scaling symmetries.

The observational viability difficulties of the dust and inverse power-law potential models, including those of tracker solutions, arise because $\lambda \to \infty$ when $\phi \to \infty$, since a large λ makes the dynamics deviate from ΛCDM dynamics. This motivates us to consider other types of scalar field potentials for which λ is globally and asymptotically regularized. For this reason, we therefore

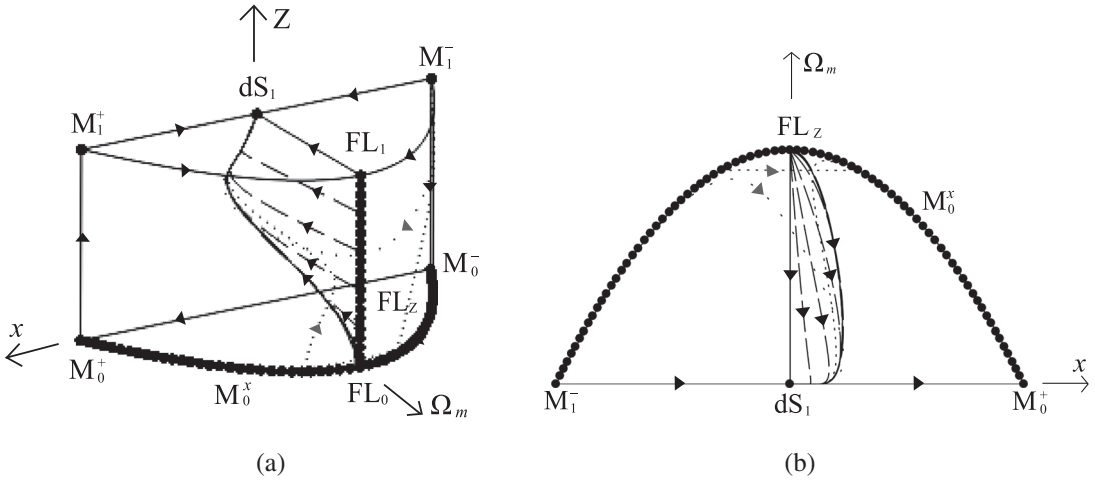

FIG. 8. The solution space of dust and an inverse power-law potential $V = V_0\phi^{-\alpha}$ with $\alpha = 1/2$. (a) (x, Ω_m, Z) state space, (b) Projection of (x, Ω_m, Z) state onto (x, Ω_m).

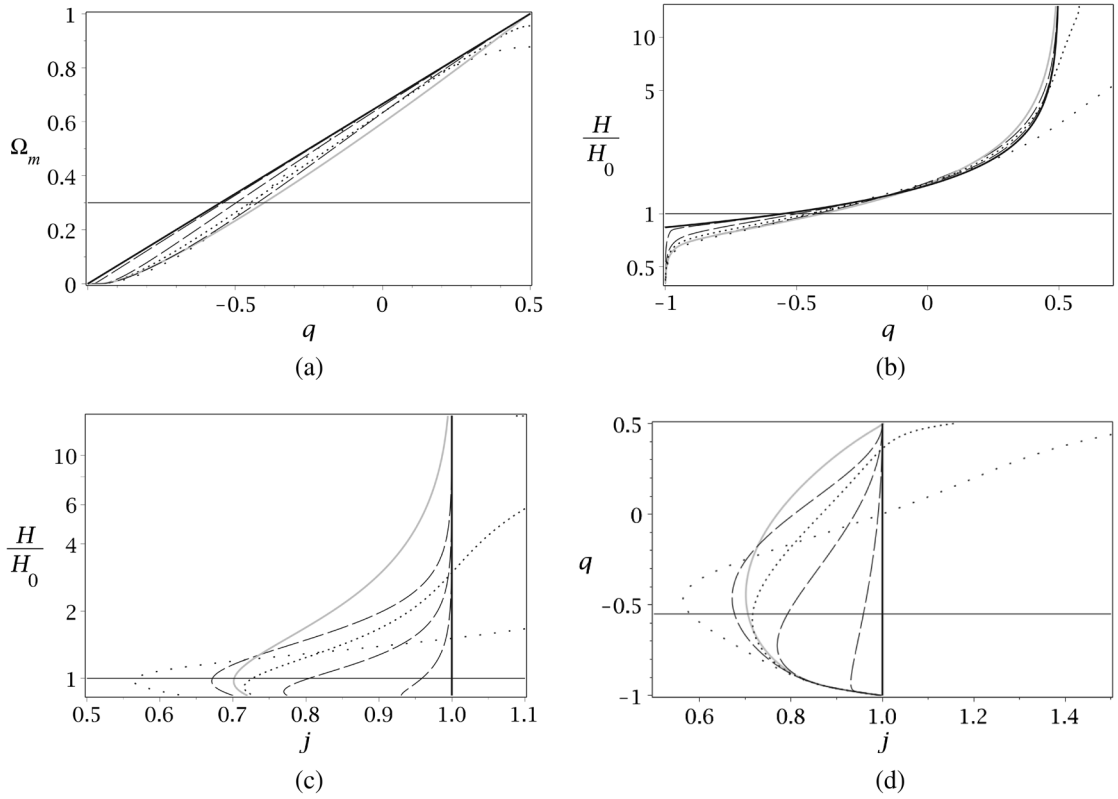

FIG. 9. Observables for dust and an inverse power-law potential $V = V_0\phi^{-\alpha}$ with $\alpha = 1/2$. The thick solid line represents ΛCDM cosmology; the horizontal lines represent now, i.e., zero redshift; and the other lines correspond to the solutions in Fig. 8, where the grey line corresponds to the tracker solution. (a) $\Omega_m - q$ diagram, (b) $h - q$ diagram, (c) $h - j$ diagram, $q - j$ diagram.

phenomenologically regularize λ of the inverse power-law potential and use (6) to derive V, in arguably the simplest possible way, so that λ becomes finite and one obtains continuous deformations of ΛCDM cosmology.

B. λ-regularization of inverse power-law potentials

To obtain a type of potential that has a regular λ and still behaves like an inverse power-law potential for large ϕ, we generalize the inverse power-law potential by choosing

$$\lambda = \frac{\alpha}{\sqrt{C^2+\phi^2}} = \frac{\lambda_{\max}}{\sqrt{1+(\phi/C)^2}}, \qquad C > 0. \tag{51}$$

Here $\lambda_{\max} = \alpha/C$ is the maximum value of $\lambda(\phi)$ while C describes the peak width of the present $\lambda(\phi)$. Using (6), this "regularized" inverse power-law $\lambda(\phi)$ leads to the potential

$$V = V_0\left(\phi + \sqrt{C^2+\phi^2}\right)^{-\alpha}. \tag{52}$$

It follows that $\lim_{\phi\to\pm\infty}(\phi^{\pm\alpha}V) = \text{const}$. Note that this class of potentials contains the inverse power-law potential by setting $C = 0$ (restricting dynamics to $\phi > 0$) and a cosmological constant by setting $\alpha = 0$. As an example, we give the potential and λ for $\alpha = 6$ and $C = 10$, depicted in Fig. 10.

The above is (so far) a purely phenomenologically motivated potential, but so was the original motivation for the inverse power-law potential [3,4]. The point here is to give a simple specific example of continuous ΛCDM scalar field deformations, illustrating features that *any* observationally viable model arising from some fundamental theory must have.

To continue we choose

$$Z = \frac{z}{1+z}, \qquad z = \phi + \sqrt{C^2+\phi^2},$$
$$\phi = \frac{z^2-C^2}{2z} = \frac{Z^2 - C^2(1-Z)^2}{2Z(1-Z)} \tag{53}$$

as the scalar field variable (here z should not be confused with the redshift). This leads to

$$\lambda = \frac{2\alpha Z(1-Z)}{Z^2 + C^2(1-Z)^2} \tag{54}$$

and the regular dynamical system

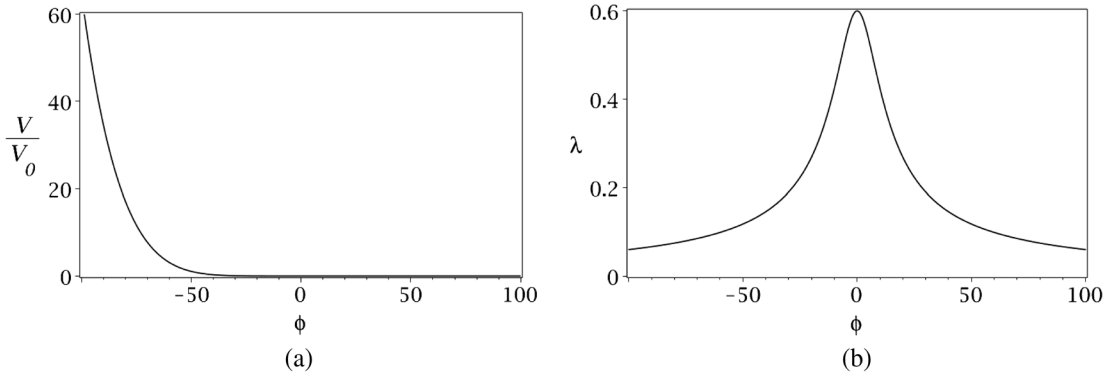

FIG. 10. The potential $V = V_0(\phi + \sqrt{C^2 + \phi^2})^{-\alpha}$ and associated $\lambda = \alpha/\sqrt{C^2 + \phi^2}$ for $\alpha = 6$ and $C = 10$. (a) Potential diagram, (b) λ diagram.

$$x' = -(2 - q)x + \sqrt{\frac{3}{2}}\lambda(Z)(1 - x^2 - \Omega_m), \tag{55a}$$

$$\Omega_m' = 3[2x^2 - \gamma_m(1 - \Omega_m)]\Omega_m, \tag{55b}$$

$$Z' = \sqrt{6}\alpha^{-1}\lambda Z(1 - Z)x = \sqrt{6}\frac{2Z^2(1 - Z)^2}{Z^2 + C^2(1 - Z)^2}x, \tag{55c}$$

where $2 - q = 3(1 - x^2) - \frac{3}{2}\Omega_m$. The qualitative properties of this system follow from the general discussion in Sec. II. We give an explicit representation of the solution space for the case $C = 10$ and $\alpha = 6$ in Fig. 11. The associated diagrams for physical observables are given in Fig. 12. As can be seen the λ-regularized models give much better results than the corresponding models with an inverse power-law potential with the same α, when C is chosen so that it is of the same order of magnitude as α, and even better if C is larger (cf. Figs. 7 and 12, which both have $\alpha = 6$). The results basically linearly improve with increasing C for a fixed α, which should not come as a surprise since $\lambda_{\max} = \alpha/C$; for $\alpha = 6$ and $C = 100$, and therefore $\lambda_{\max} = 0.06$, the dynamics for models with Ω_m close to 1 initially is almost indistinguishable from ΛCDM dynamics. Toward smaller C, the models increasingly yield similar results as the inverse power-law potential, which again is to be expected.

C. Observational λ conditions for continuous ΛCDM deformation

The structure of the flat FLRW models with dust and inverse power-law potential strongly suggests that it does not suffice to just have a monotonically decreasing potential with a shallow potential tail, since even if $\lambda \to 0$ when $\phi \to +\infty$ a large $\lambda(\phi)$ for some ϕ generally results in considerable deviations from ΛCDM cosmology. There are significant differences in the solution structure if λ is globally and asymptotically bounded or not.

This suggests that observational viability implies *global and asymptotic boundedness conditions* on λ, so that the

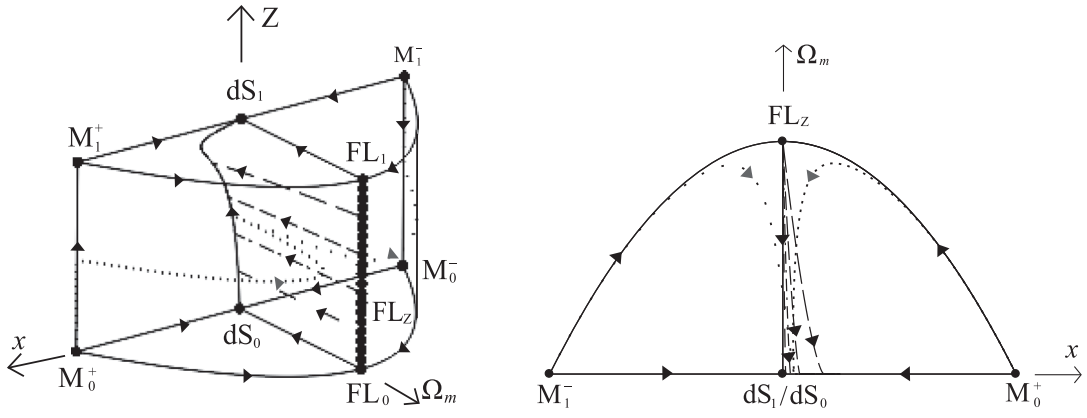

FIG. 11. Depiction of the solution space of flat FLRW models with dust and a scalar field with a potential $V = V_0(\phi + \sqrt{C^2 + \phi^2})^{-\alpha}$ and associated $\lambda = \alpha/\sqrt{C^2 + \phi^2}$ for $\alpha = 6$ and $C = 10$. (a) (x, Ω_m, Z) state space, (b) Projection of (x, Ω_m, Z) state space onto (x, Ω_m).

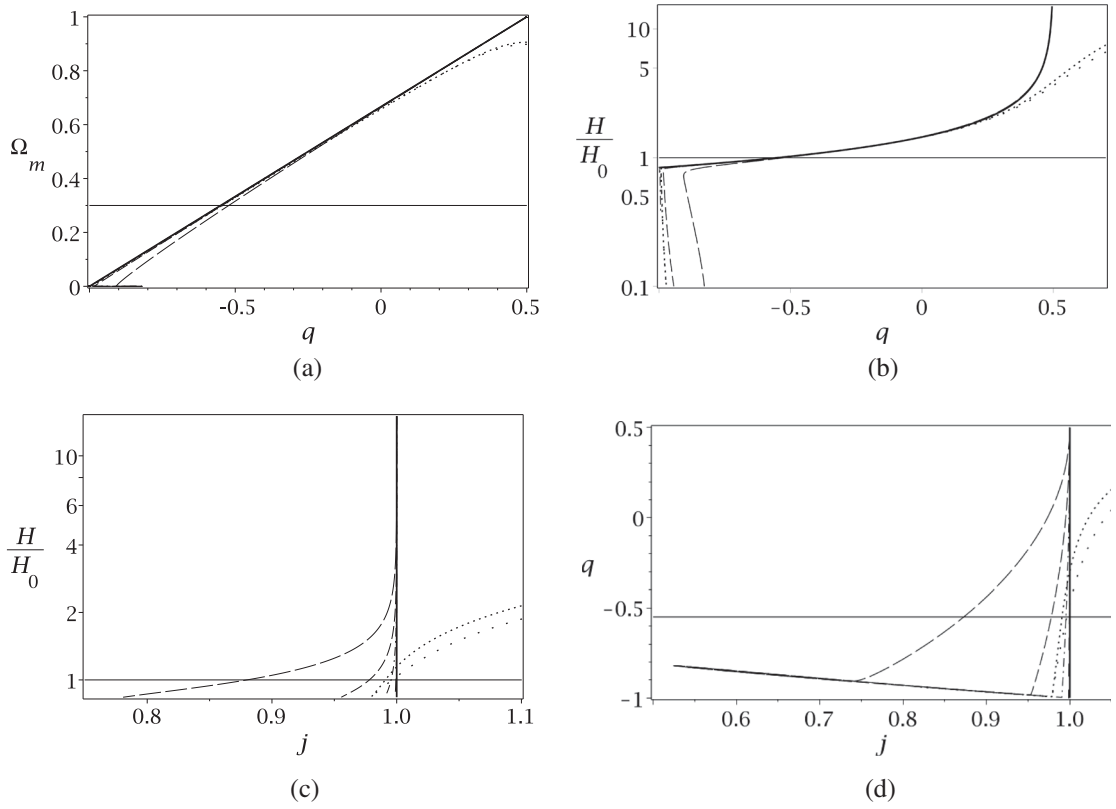

FIG. 12. Observables for flat FLRW models with dust and a scalar field with the potential $V = V_0(\phi + \sqrt{C^2 + \phi^2})^{-\alpha}$ and associated $\lambda = \alpha/\sqrt{C^2 + \phi^2}$ for $\alpha = 6$ and $C = 10$. The thick solid line represents ΛCDM cosmology; the horizontal lines represent now, i.e., zero redshift; and the other lines correspond to the solutions in Fig. 11. (a) $\Omega_m - q$ diagram, (b) $h - q$ diagram, (c) $h - j$ diagram, (d) $q - j$ diagram.

whole subset that originates from FL_Z into **S** only deviates moderately from the $x = 0$ ΛCDM surface. It should be pointed out that this not only produces an observationally viable set of models, but also alleviates the coincidence and possibly other fine-tuning problems since *all* orbits with initial values of Ω_m close to 1 behave similarly because the invariant subset that originates from FL_Z then constitutes an attracting separatrix surface, eliminating the need for any measure.[8]

ACKNOWLEDGMENTS

A. A. is supported by the projects CERN/FP/123609/2011, EXCL/MAT-GEO/0222/2012, and CAMGSD, Instituto Superior Técnico by FCT/Portugal through UID/MAT/04459/2013, and the FCT Grant No. SFRH/BPD/85194/2012. Furthermore, A. A. also thanks the Department of Engineering and Physics at Karlstad University, Sweden, for kind hospitality.

APPENDIX: A SCALAR FIELD AND TWO FLUIDS

In this work we have considered a matter content that consists of a fluid without pressure. However, the early Universe after inflation is radiation dominated and therefore somewhat more sophisticated models have both radiation and dust as matter content. In a dynamical systems context this situation can be treated as follows. Consider two noninteracting fluids with energy densities ρ_1 and ρ_2, respectively. It is then convenient to introduce

$$\rho_m = \rho_1 + \rho_2, \qquad \chi = \frac{\rho_1}{\rho_m}, \tag{A1}$$

as the two perfect fluid variables instead of ρ_1 and ρ_2.[9] Assume further that the fluids obey linear equations of state

[8] Because open sets of solutions do not follow the tracker solution closely, it was argued in [13] that solutions that were close to the tracker solution were in some sense generic due to the center manifold structures. However, such structures can be eliminated or changed by a change of variables, while the fact that there are open sets of solutions that behave quite differently than the tracker solution in terms of physical observables cannot. It is therefore a question of measures if trackerlike behavior is generic or not, and a consensus about measures seems rather unlikely. On the other hand, if center manifold structures reflect behavior in physical observables, they might very well play an important role in cosmology.

[9] For alternative ways of handling several fluids, see, e.g., [25,26].

characterized by the constant equation of state parameters γ_1 and γ_2, where we without loss of generality set $\gamma_2 > \gamma_1$ (if $\gamma_2 = \gamma_1$ we treat the problem as a single fluid). The system (9) holds for fluids with general barotropic equations of state, which includes the present case. However, having two fluids instead of one with linear equations of state makes it convenient to augment the system (9) with the additional variable χ, which leads to

$$x' = -(2-q)x + \sqrt{\frac{3}{2}}\lambda(Z)\Omega_V, \tag{A2a}$$

$$\Omega_m' = 3[2x^2 - \gamma_m(1-\Omega_m)]\Omega_m, \tag{A2b}$$

$$Z' = \sqrt{6}\frac{dZ}{d\phi}x, \tag{A2c}$$

$$\chi' = 3(\gamma_2 - \gamma_1)\chi(1-\chi), \tag{A2d}$$

where, as before, $\Omega_V = 1 - x^2 - \Omega_m$ and $\Omega_m = \rho_m/3H^2$. The deceleration parameter is given by

$$\begin{aligned} q &= -1 + 3x^2 + \frac{3}{2}\gamma_m\Omega_m \\ &= -1 + 3x^2 + \frac{3}{2}(\gamma_1\chi + \gamma_2(1-\chi))\Omega_m, \end{aligned} \tag{A3}$$

since $\gamma_m = \frac{\rho_1+\rho_2+p_1+p_2}{\rho_1+\rho_2} = \gamma_1\chi + \gamma_2(1-\chi)$. Due to the similarity with the single fluid case we choose to include the same boundaries, but with the addition of χ we also consider $\chi \in [0,1]$, where $\chi = 0$ ($\chi = 1$) corresponds to the single fluid case for ρ_2 (ρ_1).

Since $\gamma_2 > \gamma_1$ it follows that χ is strictly monotonically increasing when $0 < \chi < 1$. Furthermore, χ can be solved in terms of the scale factor a by using the conservation equation $d\rho_i/d\ln a = -3\gamma_i\rho_i$, which yields $\rho_i \propto a^{-3\gamma_i}$ and therefore

$$\chi = \frac{1}{1 + k(a/a_0)^{\gamma_1-\gamma_2}} = \frac{1}{1 + k\exp[(\gamma_1-\gamma_2)\tau]}, \tag{A4}$$

where $k = \rho_{20}/\rho_{10} = \Omega_{20}/\Omega_{10}$. It follows that $\chi \to 0$ ($\chi \to 1$) when $a \to 0$, i.e., $\tau \to -\infty$ ($a \to \infty$, i.e., $\tau \to +\infty$). Thus $\chi = 0$ in the asymptotic past and $\chi = 1$ in the asymptotic future, which tells us that the fluid with the most soft (stiff) equation of state dominates asymptotically over the other fluid at late (early) times. As a consequence of the above features it follows that asymptotic future (past) dynamics reside on the $\chi = 1$ ($\chi = 0$) subset.

Because it is possible to solve the conservation equations for each of the two fluids in terms of the scale factor, this gives rise to a constant of motion, which also reflects that the problem is really a three-dimensional one. To obtain this conserved quantity we first note that

$$\Omega_1 = \chi\Omega_m, \qquad \Omega_2 = (1-\chi)\Omega_m. \tag{A5}$$

Then, since $\rho_1 \propto a^{-3\gamma_1}$ and $\rho_2 \propto a^{-3\gamma_2}$, it follows that

$$\begin{aligned} \text{const} &= \frac{\rho_1^{\gamma_2}}{\rho_2^{\gamma_1}} \propto \frac{\Omega_1^{\gamma_2}}{\Omega_2^{\gamma_1}}(H^2)^{\gamma_2-\gamma_1} \\ &= \chi^{\gamma_2}(1-\chi)^{-\gamma_1}\Omega_m^{\gamma_2-\gamma_1}(H^2)^{\gamma_2-\gamma_1}, \end{aligned} \tag{A6}$$

where H^2 is given in terms of the state space variables in Eq. (19).

The matter subset $\Omega_m = 1$, i.e., $x = 0$, $\Omega_V = 0$, now corresponds to the two-dimensional system

$$Z' = 0, \tag{A7a}$$

$$\chi' = 3(\gamma_2 - \gamma_1)\chi(1-\chi), \tag{A7b}$$

which has the solution $Z = \text{const}$, $\chi = 1/(1 + k\exp[(\gamma_1-\gamma_2)\tau])$. The analysis of the single fluid case is directly translatable to the present context, and the line of fixed points FL_Z is now replaced with the above two-dimensional subset. It follows that the inclusion of radiation changes little of the previous discussion as regards qualitative dynamical features.

It should perhaps be pointed out that instead of χ and Ω_m it is possible to use $\Omega_1 = \rho_1/3H^2$ and $\Omega_2 = \rho_2/3H^2$ as variables, where

$$\begin{aligned} \frac{d\Omega_i}{d\tau} &= [2q - (3\gamma_i - 2)]\Omega_i, \\ q &= -1 + 3x^2 + \frac{3}{2}(\gamma_1\Omega_1 + \gamma_2\Omega_2), \end{aligned} \tag{A8}$$

and where $\Omega_V = 1 - x^2 - \Omega_1 - \Omega_2$.

[1] R. Adam *et al.* (Planck Collaboration), Planck Collaboration I, Planck 2015 results. I. Overview of products and results, arXiv:1502.01582.

[2] P. A. R. Ade *et al.* (Planck Collaboration), Planck 2015 results. XIII. Cosmological parameters, arXiv:1502.01589.

[3] P. J. E. Peebles and B. Ratra, Cosmology with a time-variable cosmological "constant", Astrophys. J. **325**, L17 (1988).

[4] B. Ratra and P. J. E. Peebles, Cosmological consequences of a rolling homogeneous scalar field, Phys. Rev. D **37**, 3406 (1988).

[5] P. J. Steinhardt, L. Wang, and I. Zlatev, Cosmological tracking solutions, Phys. Rev. D **59**, 123504 (1999).
[6] S. Tsujikawa, Quintessence: A review, Classical Quantum Gravity **30**, 214003 (2013).
[7] J. Wainwright and G. F. R. Ellis, *Dynamical Systems in Cosmology* (Cambridge University Press, Cambridge, 1997).
[8] A. A. Coley, *Dynamical Systems and Cosmology* (Kluwer Academic Publishers, Dordrecht, 2003).
[9] S. Weinberg, *Cosmology* (Oxford University Press, Oxford, 2008).
[10] R. Giambo and J. Miritzis, Energy exchange for homogeneous and isotropic universes with a scalar field coupled to matter, Classical Quantum Gravity **27**, 095003 (2010).
[11] C. Uggla, Global cosmological dynamics for the scalar field representation of the modified Chaplygin gas, Phys. Rev. D **88**, 064040 (2013).
[12] G. Leon and C. R. Fadragas, *Cosmological Dynamical Systems and Their Applications* (LAP LAMBERT Academic Publishing, 2012).
[13] N. Tamanini, Dynamical systems in dark energy models, Ph.D. thesis, University College, 2014.
[14] A. Alho and C. Uggla, Global dynamics and inflationary center manifold and slow-roll approximants, J. Math. Phys. (N.Y.) **56**, 012502 (2015).
[15] A. Alho, J. Hell, and C. Uggla, Global dynamics and asymptotics for monomial scalar field potentials and perfect fluids, Classical Quantum Gravity **32**, 145005 (2015).
[16] R. D. Blandford, M. Amin, E. A. Baltz, K. Mandel, and P. J. Marshall, Cosmokinetics, Observing Dark Energy, ASP Conference Series **339**, 27 (2005).
[17] D. Rapetti, S. W. Allen, M. A. Amin, and R. D. Blandford, A kinematical approach to dark energy studies, Mon. Not. R. Astron. Soc. **375**, 1510 (2007).
[18] E. J. Copeland, A. R. Liddle, and D. Wands, Exponential potentials and cosmological scaling solutions, Phys. Rev. D **57**, 4686 (1998).
[19] A. Nunes and J. P. Mimoso, On the potentials yielding cosmological scaling solutions, Phys. Lett. B **488**, 423 (2000).
[20] C. Uggla, R. T. Jantzen, and K. Rosquist, Exact hypersurface-homogeneous solutions in cosmology and astrophysics, Phys. Rev. D **51**, 5522 (1995).
[21] J. M. Heinzle and C. Uggla, Monotonic functions in Bianchi models: Why they exist and how to find them, Classical Quantum Gravity **27**, 015009 (2010).
[22] S. C. C. Ng, N. J. Nunes, and F. Rosati, Applications of scalar attractor solutions to cosmology, Phys. Rev. D **64**, 083510 (2001).
[23] L. A. Urena-Lopez, Unified description of the dynamics of quintessential scalar fields, J. Cosmol. Astropart. Phys. 03 (2012) 035.
[24] Y. Gong, The general property of dynamical quintessence field, Phys. Lett. B **731**, 342 (2014).
[25] A. A. Coley and J. Wainwright, Qualitative analysis of two-fluid Bianchi cosmologies, Classical Quantum Gravity **9**, 651 (1992).
[26] J. M. Heinzle, N. Röhr, and C. Uggla, Matter and dynamics in closed cosmologies, Phys. Rev. D **71**, 083506 (2005).